FFI Norwegian Defence Research Establishment

21/00110

FFI-RAPPORT

The impact angle dependency of a piezoelectric impact sensor

– a conceptual study

Jarl Øystein Samseth

The impact angle dependency of a piezoelectric impact sensor
— a conceptual study

Jarl Øystein Samseth

Norwegian Defence Research Establishment (FFI) 26 March 2022

Keywords
Akustiske sensorer
Piezoelektrisitet
Sjokkbølger
Brannrør

FFI report
21/00110

Project number
1462

Electronic ISBN
978-82-464-3402-5

Approvers
Hege Jødahl, *Research Manager*
Arne Petter Bartholsen, *Director of Research*

The document is electronically approved and therefore has no handwritten signature.

Summary

Piezoelectric impact sensors are designed to trigger an immediate or delayed detonation when they sense that the projectile impacts a desired target. The initial voltage signal of a piezoelectric element (PE) in a projectile depends on several conditions: the target (material properties, thickness etc.) and terminal ballistic parameters (impact speed and impact angle). This report presents a conceptual study of the PE generated (PEG) charge as function of the impact angle. The PEG charge signal will be derived in the case when a longitudinal, plane, square-shaped stress pulse enters the PE. A pulse of that form resembles the simplest form of shock waves, and it will simplify the piezoelectric equations.

Four factors that reduce the PEG charge and PE voltage as the impact angle increases, are considered: (1) the collision impulse which generates the stress pulse at impact, (2) the transmission coefficient, (3) the electric field dependence on the stress pulse's amplitude and direction as described by the piezoelectric equations, and (4) the proportion of the PE's volume effectively being stressed by the stress pulse that traverses it. Other effects are discussed qualitatively, but are either regarded as negligible or too complex for this simple analytical study to be included in the final PEG charge formula.

The derived PEG charge formula is applied to a simple scenario where all the assumptions in the derivation are true, and where the stress pulse's incident angle equals the impact angle. Though this scenario is mainly for conceptual study purposes, it also resembles a special case: when the side of a (e.g. conically shaped) projectile nose collides with a flat and equally angled target plate and generates a plane shock wave. The projectile nose shape ensures that a plane, square pulse is produced at the impact interface and propagates unchanged into a PE made of a PZT material, where the stress generates an electric field.

In this scenario the relative PEG charge amplitude decreases approximately linearly (though with a contribution from a cosine factor), as the impact angle increases. The PEG charge at 60° impact angle is $Q(60^\circ) \approx 0.2 \cdot Q(0^\circ)$. We also learn that the angle dependency of a closed circuited PE is quite similar to that of an open circuited PE.

The shape of the PEG charge signal's rising edge as a stress pulse enters it at an angle, is also studied. As the transmission angle increases, the rising edge changes from a straight line to an S-shape.

Sammendrag

Piezoelektriske anslagssensorer designes for å trigge en øyeblikkelig eller forsinket detonasjon idet de måler at prosjektilet treffer et ønsket mål. Spenningssignalet initielt fra et piezoelektrisk element i et prosjektil avhenger av flere forhold: målet (dets materielle egenskaper, tykkelse osv.) og terminalballistiske parametre (anslagsfart og anslagsvinkel). I denne rapporten presenteres en konseptuell studie av ladningen generert av (og spenningen over) et piezoelektrisk element som funksjon av anslagsvinkel. Det piezoelektriske elementets genererte ladningssignal blir utledet for et tilfelle der en longitudinal, plan og firkantformet trykkpuls entrer det piezoelektriske elementet. En slik puls ligner på den enkleste formen for sjokkbølger, og benyttes her fordi den forenkler de piezoelektriske ligningene.

Fire faktorer reduserer den genererte ladningen og spenningen når anslagsvinkelen øker: (1) den genererte trykkamplituden ved anslag som er gitt av impulsen ved anslag, hvilket er proporsjonalt med den komponenten av prosjektilets bevegelsesmengde som peker vinkelrett på målplata, (2) transmisjonskoeffisienten, (3) det elektriske feltets avhengighet av trykkpulsens amplitude og retning som beskrevet av de piezoelektriske ligningene, og (4) volumandelen av det piezoelektriske elementet som effektivt sett blir stresset av den kryssende trykkpulsen. Andre effekter er også diskutert kvalitativt, men er enten neglisjerbare eller for komplekse for denne analytiske studien til å bli inkludert (kvantitativt) i den fullstendige ligningen for den genererte ladningen i det piezoelektriske element.

Den utledede formelen for den genererte ladningen blir anvendt på et enkelt scenario der alle antagelsene i utledningen er gjeldende, og der trykkpulsens innkommende vinkel på det piezoelektriske elementet er lik anslagsvinkelen. Selv om dette scenarioet hovedsakelig studeres for konseptuell forståelse, så ligner den også på et spesialtilfelle: når en flat, skråstilt målplate og (den eksempelvis konisk formede) prosjektilnesas like skråstilte sideflate kolliderer med hverandre og genererer en plan sjokkbølge. Prosjektilnesas form er slik at den produserer en plan, firkantpuls i kollisjonsflaten som får propagere uforandret frem til det piezoelektriske elementet, hvor stresspulsen genererer et elektrisk felt.

Scenarioet viser at den relative ladningssamplituden avtar tilnærmet lineært (med et bidrag fra en cosinusfaktor) etterhvert som anslagsvinkelen øker. Ved 60° anslagsvinkel har ladningen falt til $Q(60^\circ) \approx 0.2 \cdot Q(0^\circ)$. Vi ser også at vinkelavhengigheten er ganske lik for et piezoelektrisk element i lukket krets og i åpen krets.

Formen på den stigende flanken i ladningssignalet etter hvert som en stresspuls entrer det piezoelektriske elementet på skrått, er også studert. Med økende transmisjonsvinkel endrer stigningen seg fra en rett linje til en S-kurve.

Contents

1 Introduction

This report is part of a project where the goal is to understand piezoelectric impact sensors in the nose of projectiles. A piezoelectric impact sensor consists of a piezoelectric element (PE) and an electric circuit to trigger detonation or notify when the projectile has hit/impacted an object of sufficient stiffness and thickness (i.e. desired targets). A PE is an element made of a material that produces an electric field when mechanically stressed (compressed, stretched or bended), and vice versa [2].

The PE voltage signal depends on several collision conditions: the target (material properties, thickness etc.) and terminal ballistic parameters (impact speed and impact angle). In order to detect desired targets and distinguish them from other targets, the terminal ballistic parameters must be accounted for. Both the impact speed and impact angle are significant to the PE voltage signal of an impact sensor. The stress generated at impact is known to increase with increasing impact speed (in both elastic and inelastic/plastic collisions) [9]. As we shall see, the PE voltage is a function of the impact angle. The present report is an analytical approach to conceptually study this angle dependency.

In the present study we will see that four angle dependent factors affect the amount of charge generated in the PE:

- **Impulse**: The stress pulse amplitude generated at the impact interface is given by the collision impulse.
- **Transmission coefficient**: The proportion of the stress pulse amplitude that is transmitted into the PE, depends on the angle of the incident stress pulse.
- **Piezoelectric effect**: The piezoelectric equations relate the stress vector to the electric field. The stress vector direction is of importance.
- **Stressed area coverage**: The angle at which the incident stress pulse enters the PE, affects how much of the PE is effectively stressed.

The following chapters will introduce one factor each. They will bring us along on the stress pulse's journey from being generated at the impact interface, to transmission into the PE where it generates voltage and charge by means of the piezoelectric effect. The last chapter (chapter 6) will combine all the four factors into one PE generated charge expression as function of impact angle, and apply it to a simple scenario.

2 Impulse: Stress generated by impact

In this chapter we will introduce the impact angle and its effect on the generated stress pulse amplitude during an oblique collision. The stress pulse is generated by an impact impulse. The momentum is conserved at impact between two slabs of materials as they collide. The impulse is the change in momentum over time:

$$\frac{\Delta(m_A\vec{u}_A + m_B\vec{u}_B)}{\Delta t} = 0 \tag{2.1}$$

This is another way of stating that any force has its counterforce: $\vec{F} = -\vec{F}^*$ (Newton's third law).

The force at impact is orthogonal to the interface between the two materials. When a projectile impacts a plate at an angle α with impact velocity $\vec{u}$, the force amplitude F becomes

$$\begin{aligned}\vec{F} &= F\hat{n} = \frac{\mathrm{d}(m\vec{u})}{\mathrm{d}t} \\ F &= \frac{\mathrm{d}(m\vec{u})}{\mathrm{d}t}\cdot\hat{n} = m\frac{\mathrm{d}(u)}{\mathrm{d}t}\cos\alpha\end{aligned} \tag{2.2}$$

where $\hat{n}$ is the impact interface's normal vector.

Since stress in the target plate and projectile is generated by the external pressure on the impacting interface, the stress amplitude $\sigma_0(\vec{r},\alpha) = F/A$ is proportional to cosine of the impact angle α. The PE voltage will scale accordingly, as we shall see in chapter 6. Let's call this scaling factor

$$I = \frac{\sigma_0(\alpha)}{\sigma_0(0)} = \cos\alpha \tag{2.3}$$

2.1 Generated pulse shape

Different geometries of the impact interface generate different stress pulses. In this study we will look at a type of stress pulse that simplifies the piezoelectric equations: a pulse with the same stress vector (i.e. the same stress amplitude and direction) everywhere in the pulse. This is the case for a plane, square pulse. A plane wave is generated when the impact interface is flat.

A square pulse is a square shaped pulse along the pulse's propagation direction, as illustrated in fig. 2.1.

A plane stress pulse (or wave) is a pulse where the stress vectors everywhere in the pulse point in the same direction and the stress is uniform in the plane perpendicular to the propagation direction. In other words the stress vector of a plane stress wave that propagates in the z-direction, is independent of x and y: $\vec{\sigma}(\vec{r}(t)) = \vec{\sigma}(z(t))$. Equivalently, a plane stress pulse has regions of equal stress where each region constantly form a plane in three dimensional space, as illustrated in fig. 2.2. Hence the expression '*plane* pulse'.

A sound wave or a longitudinal shock wave is generated at the impact interface, depending on the impact impulse relative to the material's elastic limit [9]. A sound wave is a longitudinal, elastic wave. 'Longitudinal' means that the particle velocity and the stress vector point along the wave's propagation direction.

A longitudinal, plane, square stress pulse is sketched as a shaded area in fig. 2.3. The stress vector $\vec{\sigma} = \sigma_0 \cdot \hat{z}$ is the same everywhere in the pulse. The hat on $\hat{z}$ denotes a unit vector.

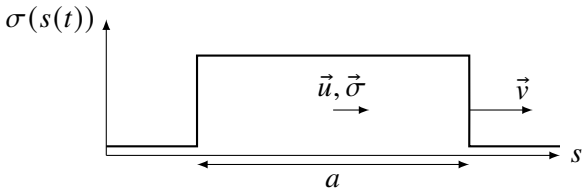

Figure 2.1 *A square stress pulse propagating at velocity $\vec{v}$ along an arbitrary axis $\vec{s}$. It has particle velocity $\vec{u}$ and stress vector $\vec{\sigma}$ everywhere in the pulse.*

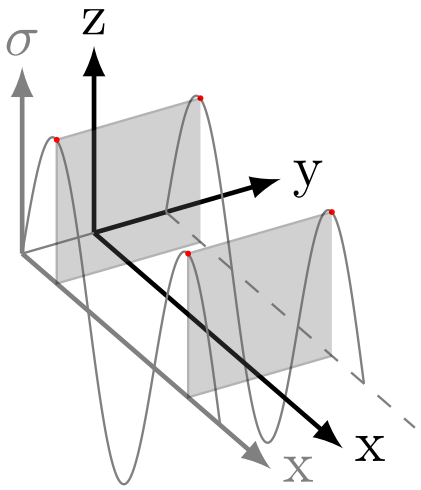

Figure 2.2 *A plane sine wave has regions of equal stress (marked with red dots) that form planes (shaded areas) in three dimensional space. Here the stress wave oscillates along the x-axis in the xy-plane.*

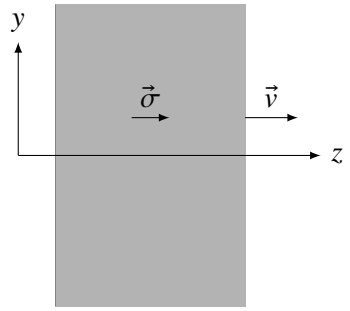

Figure 2.3 *A longitudinal, plane, square stress pulse is propagating in the z-direction with velocity $\vec{v}$. Its stress vector $\vec{\sigma}$ is constant everywhere in the pulse (the shaded area), pointing in the same direction as the pulse's velocity.*

2.2 Effective target thickness and deformations

As a projectile penetrates a target in an inelastic collision, the generated stress pulse will most likely change during the course of penetration due to deformations. Deformations will change the size and shape of the impact interface. The greater the impact interface area, the smaller the pressure. The size of the impact interface area may vary with the impact angle, but it also depends on the (initial) shape of the projectile and the target. A flat target may envelop a ball that penetrates it, and its spherical symmetry makes the impact interface area independent of the impact angle. A rod, on the other hand, has different surfaces in different directions and will thus be enveloped differently depending on the angle of impact.

The generated stress pulse also depends on the collision duration and the mass that the projectile effectively has to accelerate as it penetrates or perforates the target. The amount of mass depends on the projectile's impact angle, as the projectile's line of flight has an effective target thickness in its path.

These effects are too complex to be quantitatively described in this analytical study, and will therefore be neglected in the relative PE voltage amplitude that we are deriving, even though they are likely to be significant during penetration. That being said, these effects may be small at the very beginning of the collision, because the (plastic) deformations take time to develop and envelop.

3 Transmission and refraction

This chapter presents the transmission coefficient, Snell's law for refraction and how the transmission coefficient depends on the electric circuit that the PE is connected to.

Transmission coefficient

When a stress wave crosses the interface from material A to B, the stress amplitude and the propagation direction are governed by Newton's third law and the proposition that the materials/particles at each side of the interface have equal velocities orthogonally to the interface at all times. The ratio between transmitted and incident stress is called transmission coefficient T. The reflection coefficient R is defined correspondingly.

For an incident longitudinal wave in material A propagating at an angle θ_A relative to the normal surface vector of material B, the stress transmission ratio is

$$T = \frac{2Z_B/\cos\theta_B}{Z_A/\cos\theta_A + Z_B/\cos\theta_B} \tag{3.1}$$

$$= 2\left(\frac{Z_A}{Z_B}\frac{\cos\theta_B}{\cos\theta_A} + 1\right)^{-1}$$

$$R = \frac{Z_B\cos\theta_A - Z_A\cos\theta_B}{Z_A\cos\theta_B + Z_B\cos\theta_A} \tag{3.2}$$

$$1 + R = T \tag{3.3}$$

where the mechanical impedance $Z_j = \rho_j \cdot v_j$ for longitudinal waves in a material labelled j [15]. ρ is the mass density. v is the stress wave's speed.

The speed of sound for elastic, longitudinal waves is

$$v = \sqrt{Y/\rho} \tag{3.4}$$

where Y is Young's modulus. The speed v of shock waves is given by the Hugoniot equation $v = C + su$, where C and s are constants derived from linear regression on empirical data [9]. u is the particle speed.

Refraction

When the wave in medium A is incident at an angle θ_A to the interface's normal line (illustrated in fig. 3.1), the transmitted wave refracts and propagates at an angle θ_B into medium B. According to Snell's law the angles of transmitted ray θ_B and incoming ray $\theta_{A,i}$ are related as

$$\frac{\sin\theta_{A,i}}{v_A} = \frac{\sin\theta_B}{v_B} \tag{3.5}$$

where v_A and v_B are the stress wave speeds in medium A and B, respectively. The reflected ray has the same, but negative, angle as the incoming ray: $\theta_A = \theta_{A,i} = -\theta_{A,R}$. Snell's law is illustrated in fig. 3.1.

The maximum transmission angle θ_B is the angle where the incident angle $\theta_{A,i}$ is 90°. For longitudinal waves transmitted from steel into a PE made of Noliac NCE56, $\max\theta_B = \sin^{-1}(v_{PE}/v_A) = 41°$ for an open circuited PE and 27° for a short circuited PE. The material data are presented in table 3.1.

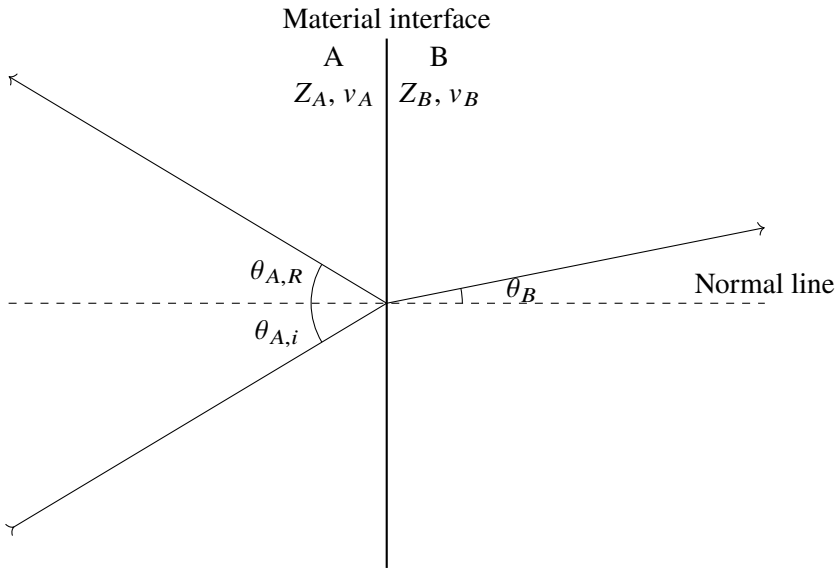

Figure 3.1 Snell's law illustrated. The refraction index for stress waves is the sound of speed v in each material.

Material	Young's modulus Y GPa	Mass density ρ kg/m^3	Speed of sound v m/s
Steel Ovako SS2541 [4]	210	7800	5189
Noliac NCE56, open circuit (D=0) [3]	92.6	7650	3479
Noliac NCE56, short circuit (E=0) [3]	41.8	7650	2338

Table 3.1 Material properties for PE and steel. Speed of sound is calculated using eq. (3.4).

3.1 Transmission into an open vs. short circuited PE

A PE's elasticity depends on its material properties and on the electric circuit of which it is a part. Strain induces electric fields in PEs by (further) polarising the material [2]. If such polarisation causes an electric current, some mechanical energy is transferred into the electric circuit, and this softens the PE. Therefore a PE in an open circuit is stiffer than in a short circuit. The Young's modulus ratio between a short circuited and an open circuited PE, is $Y_E/Y_D = (1 - k_{33}^2)$ in the PE's polarisation direction[1], where k_{33} is the electromechanical coupling factor of the PE in that direction [2]. A closed circuit with some electric impedance causes an elasticity somewhere between the elasticity of an open and a short circuited PE.

If you want to calculate the stiffness matrix of an open circuited PE from that of a short circuited PE, or vice versa, take a look at appendix A.

The ratio between transmission into an open and a short circuited PE, is

$$T_D/T_E = \frac{Z_A + Z_{PE,E}}{Z_A + Z_{PE,D}} \cdot \frac{Z_{PE,D}}{Z_{PE,E}} \tag{3.6}$$

at 0° incident angle. $Z_{PE,D}$ and $Z_{PE,E}$ are the mechanical impedances of open and short circuited PEs, respectively.

The ratio between the refraction angle's of an open and a short circuited PE, is

$$\frac{\sin\theta_{B,D}}{\sin\theta_{B,E}} = \frac{v_{B,D}}{v_{B,E}} = \sqrt{1/(1 - k_{33}^2)} \tag{3.7}$$

The transmission of sound from steel into a PE made of Noliac's PZT material NCE56, is 1.29 times greater in an open circuit than in a short circuit. And the sine of the refraction angle is 1.49 times greater. NCE56 has $k = 0.74$ [3], so $(1 - k_{33}^2) = 0.45$. This is calculated from eq. (3.6) and eq. (3.7) using data from table 3.1.

PEs are orthotropic

The structure and elasticity of piezoelectric materials are anisotropic (typically orthotropic, like PZT crystallites [2]). In this report the isotropic transmission coefficient presented in eq. (3.1), will be used as an approximation. We choose the elasticity component in the PE's polarisation direction, since Snell's law is deduced from the proposition that the particle velocities *orthogonal* to the interface, are equal on both sides of the interface. The Young's modulus in that direction is s_{33}^{-1} in datasheets [3], where s is the PE material's elastic compliance matrix. The polarisation direction is typically indexed as direction 3.

[1]The annotations: subscript D annotates open circuited PEs (where the displacement field $\vec{D} = 0$), and E annotates short circuited PEs (where the electric field $\vec{E} = 0$).

4 The piezoelectric effect

In this chapter we will study the expected PE voltage and charge output as a square stress pulse traverses a PE at an angle θ_T relative to the PE's polarisation direction. First we study how the electric field depends on the stress vector's direction. Then we derive the voltage amplitude for a line-segment of the PE parallel to its polarisation direction before we integrate all these infinitesimal line-segments into an expression for the entire PE's voltage. At last a more general expression of the charge generated in open, closed and short circuited PEs, is derived.

Piezoelectricity is the material property where electric charge is generated on the material's surface when the material is mechanically stressed, and vice versa [2]. Piezoelectric materials are ferroelectric, which is a class of dielectric materials that can be polarised (dipoles are formed) in the absence of an electric field [10]. For example in the piezoelectric ceramic made of lead zirconate titanate (PZT) the lattice can be deformed by electric field or by stress, which moves the centre atom titanium (Ti) or zirconium (Zr) and generates a dipole. See the lattice cell in fig. 4.1. Due to the atoms' different electronegativity, an anisotropic structure is a polarised structure.

Net unpolarised PZT ceramics consist of (grains of) lattice cells with randomly oriented polarisations [17, p. 248]. The dipole orientation of these cells are aligned in a process called the poling process by applying a strong electric field to the PE, as sketched in fig. 4.2. This process results in a permanent, net polarisation when the external electric field is removed [17, p. 248].

An electric field is produced in an open circuited PE when it is stressed, and vice versa. The relation between the stress and the electric field at an infinitesimal element anywhere in the PE, is given by the piezoelectric equations.

The linear piezoelectric equations of states have been derived by Haskins and Hickman [12]. Mason [14] deduced higher order piezoelectric equations of states. The adiabatic, linear piezoelectric equations are:

$$\vec{S} = \underline{s}\vec{\sigma} + \underline{d}^T \vec{E} \tag{4.1}$$

$$\vec{D} = \underline{d}\vec{\sigma} + \underline{\varepsilon}\vec{E} \tag{4.2}$$

according to the IEEE Standard from 1987 [17]. Strain $\vec{S}$ and stress $\vec{\sigma}$ are both 6×1 vectors according to the Voigt notation: $\vec{\sigma} = [\sigma_1, \sigma_2, \sigma_3, \sigma_4, \sigma_5, \sigma_6]^T = [\sigma_{11}, \sigma_{22}, \sigma_{33}, \sigma_{23}, \sigma_{31}, \sigma_{12}]^T = [\sigma_x, \sigma_y, \sigma_z, \sigma_{yz}, \sigma_{zx}, \sigma_{xy}]^T$ and likewise for strain. The last three elements are shear strain/stress

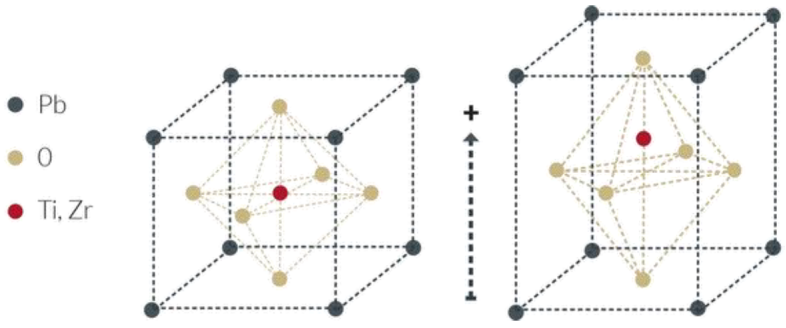

Figure 4.1 The lattice cell structure of (left) isotropic and depolarised PZT and (right) orthotropic and polarised PZT. It is depolarised above the Curie temperature. The figure is copied from [2].

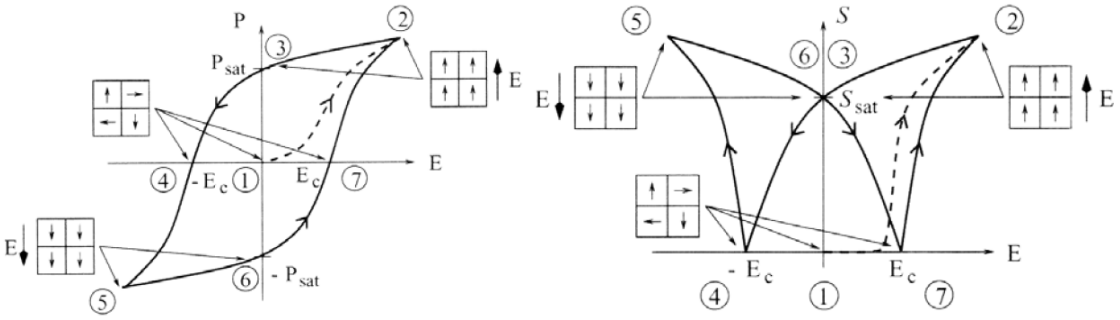

Figure 4.2 The sketched hysteresis loops of (left) polarisation and (right) strain for a PZT ceramic. The hysteresis loops are induced by loading the PE with a cycling electric field. The first load start at origin (number 1) and follows the dashed line until the PE is polarised (the poling process), where the domains of dipoles are all aligned. Then, when the electric field is reduced, the PE state follows the curve from (2) to (3) where the PE is permanently polarised and saturated (P_{sat}). The numbers indicate the different domain states: The dipole orientations are sketched with arrows in the domain boxes. The figure is copied from [20], based on measurements by [19].

elements. $\vec{E} = [E_x, E_y, E_z]^T = [E_1, E_2, E_3]^T$ is the electric field, and $\vec{D}$ is the corresponding three-dimensional displacement field vector.

The subscripts denote the directions in the anisotropic PE: 3 means the PE's polarisation direction (here oriented in the z-direction) in typical datasheets like from Noliac [3], so 1, 2 and 3 means x-, y- and z-direction, respectively. Superscript T denotes that the matrix is transposed. $\underline{\varepsilon}$ is the permittivity matrix. It is a diagonal matrix with elements $\varepsilon_1, \varepsilon_2$ and ε_3. $\underline{d}$ is the 6×3 piezoelectric charge matrix and $\underline{s}$ is the 6×6 elastic compliance matrix. The elastic compliance matrix is the inverse stiffness matrix. Linear elasticity is assumed. The diagonal elements s_{11}, s_{22} and s_{33} are the inverse Young's moduli in all three directions. Typical matrices for materials like PZT ceramics, are

$$\underline{d} = \begin{bmatrix} 0 & 0 & 0 & 0 & d_{15} & 0 \\ 0 & 0 & 0 & d_{24} & 0 & 0 \\ d_{31} & d_{32} & d_{33} & 0 & 0 & 0 \end{bmatrix}, \; \underline{s} = \begin{bmatrix} s_{11} & s_{12} & s_{13} & 0 & 0 & 0 \\ s_{21} & s_{22} & s_{23} & 0 & 0 & 0 \\ s_{31} & s_{32} & s_{33} & 0 & 0 & 0 \\ 0 & 0 & 0 & s_{44} & 0 & 0 \\ 0 & 0 & 0 & 0 & s_{55} & 0 \\ 0 & 0 & 0 & 0 & 0 & s_{66} \end{bmatrix}$$

It is important to note that these linear constitutive equations only hold true in a limited range for PZT-materials due to hysteresis and creep [2]. They are linear approximations to the non-linear piezoelectric effect. The hysteresis loops in fig. 4.2 show the non-linear (reverse) piezoelectric effect.

The definition of the displacement field for dielectric materials is

$$\vec{D} = \varepsilon_0 \vec{E} + \vec{P} \tag{4.3}$$

with polarisation $\vec{P}$ and the permittivity in vacuum ε_0. All equivalent combinations of piezoelectric equations of states can be derived from eq. (4.1), eq. (4.2) and eq. (4.3) [12].

The charge in a PE can be calculated from eq. (4.2) by Gauss' law. Gauss' law states that the total, free and bound charge inside a closed surface equals the integrated divergence of the electric field E, the displacement field D and the polarisation P, respectively:

$$Q_t = \oint \varepsilon_0 \vec{E}\, \mathrm{d}\vec{A} \tag{4.4}$$

$$Q_f = \oint \vec{D}\, \mathrm{d}\vec{A} \tag{4.5}$$

$$Q_b = -\oint \vec{P}\, \mathrm{d}\vec{A} \tag{4.6}$$

The total charge in a system is the sum of the free charge and the bound charge, where the bound charge is the equivalent charge bound to one of the poles of a dipole. When applying Gauss' laws eq. (4.4), (4.5) and eq. (4.6) to eq. (4.3), we get

$$Q_t = Q_f + Q_b \tag{4.7}$$

There are various electric circuit conditions that affect the PE's behaviour. In this report we will only consider a PE in sensor mode, which means that the PE is only polarised by stress, like for example in a microphone. Another possible mode is the actuator mode, where the PE is only polarised by applied electric field, like in a speaker. The PE can also be in a combination of the two modes where both mechanical stress and electric field are applied to the PE, like in an ultrasound equipment. The PE mode depends on whether there is any voltage sources in the electric circuit other than the PE. In sensor mode the PE can be in an open, closed (i.e. connected to other components) or short circuit.

4.1 The free charge in a stressed, short circuited PE

For a short circuited (SC) PE the net electric field $\vec{E}$ is constantly zero [2]. This is because the voltage across it instantaneously becomes zero, assuming that the electric impedance in the circuit is negligible. In that case the displacement field D is only a function of the stress according to eq. (4.2):

$$\vec{D}_{\mathrm{SC}} = \underline{d}\vec{\sigma} \tag{4.8}$$

According to Gauss' law, the corresponding free charge is

$$Q_f = \int \sum_{i=1}^{3} d_{3i}\sigma_{ii}\mathrm{d}A_3 \tag{4.9}$$

in a PE with parallel electrodes that are orthogonal to the polarisation direction. A_3 is a cross section area in the PE with a normal vector along the polarisation direction (axis 3). The displacement field flux is integrated over the entire Gaussian surface to find the free charge (on the electrode surfaces) that the Gaussian surface envelopes, as illustrated in fig. 4.3a.

We should get the same free charge Q_f in the electrodes from eq. (4.9) regardless of where the cross section area A_3 is located along the z-axis, i.e. regardless of where the stress is integrated in

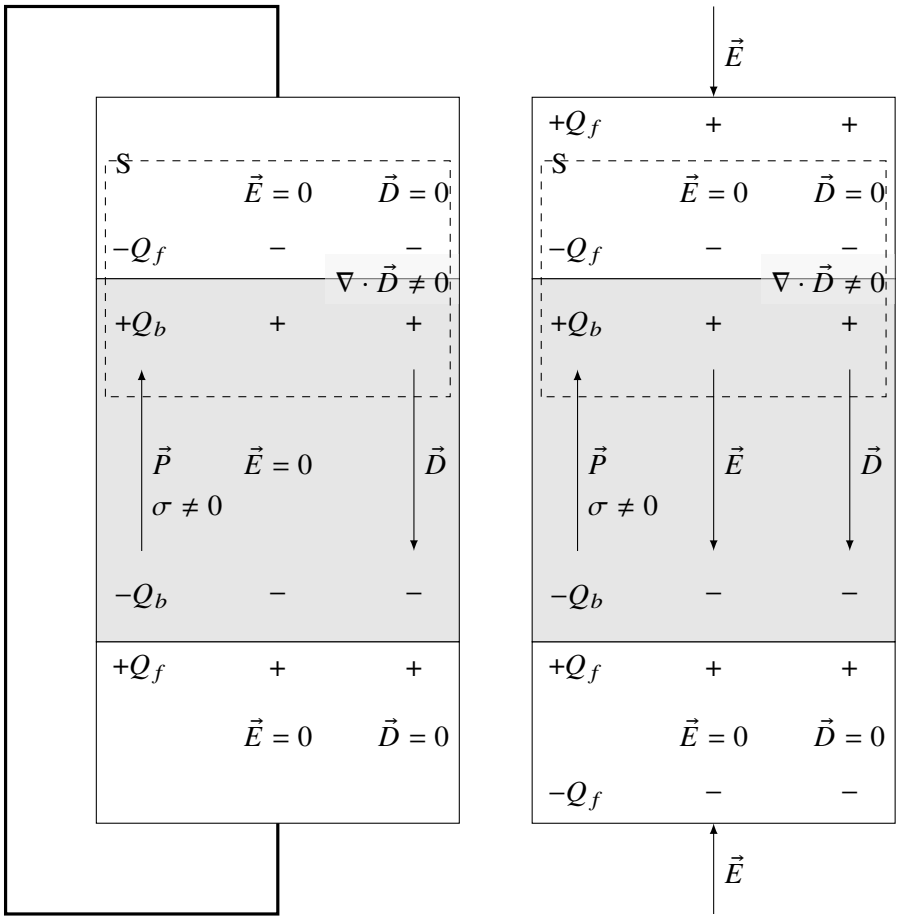

(a) Short circuited PE *(b) Open circuited PE*

Figure 4.3 The polarisation $\vec{P}$, electric field $\vec{E}$, displacement field $\vec{D}$, bound charge Q_b and free charge Q_f are presented for (a) a stressed, short circuited PE at voltage equilibrium and (b) a stressed, open circuited PE at voltage equilibrium. The piezoelectric material (grey square) is located in between two electrodes (white squares). A Gaussian surface S that envelopes the bound and free charge, is drawn as a dashed square.

the PE. Therefore the local stress at position z can be replaced by the average stress $\bar{\sigma}$ of the entire PE:

$$Q_f = A_e \sum_{i=1}^{3} d_{3i} \bar{\sigma}_{ii} \tag{4.10}$$

A_e is the electrode area.

The bound charge is equal to the negative free charge ($Q_f = -Q_b$) in a short circuited PE because the total charge is zero ($Q_t = 0$) in eq. (4.7). The total charge is zero because the electric field on the Gaussian surface in eq. (4.4) is zero. The opposite sign in $Q_f = -Q_b$ means that the electrodes have the opposite polarity of the dipoles in the short circuited PE. The bound charge attracts free charge to the electrodes.

4.2 The free charge and electric field in a stressed, open circuited PE

The displacement field $\vec{D}$ is regarded as constant in time ($\frac{\partial D}{\partial t} = 0$) in an open circuited (OC) PE [2], while the stress and electric field may vary in the PE. The free charges (the electrons) in the highly conducting electrodes immediately respond to any changes in the electric field until voltage equilibrium is attained. The boundary condition for an open circuited PE is therefore that $E = 0$ and $D = 0$ inside the electrodes at voltage equilibrium, as illustrated in fig. 4.3b.

Inside the piezoelectric material $D \neq 0$ at voltage equilibrium because $D = 0$ in the electrodes and the divergence of $\vec{D}$ is non-zero ($\nabla \cdot \vec{D} \neq 0$) at the surface of the electrodes where the free charge has accumulated. According to eq. (4.2), the electric field inside the open circuited PE is given by the displacement field and the stress that is present:

$$\vec{E}_{\mathrm{OC}} = \underline{\varepsilon}^{-1} \vec{D}_{\mathrm{OC}} - \underline{\varepsilon}^{-1} \underline{d} \vec{\sigma} \tag{4.11}$$

The voltage across a homogeneously stressed open circuited PE is therefore a function of two terms: the stress *and* the displacement field. The voltage is generally defined as

$$V_{\mathrm{PE}}(t) = -\int_0^L \vec{E}(\vec{r}, t)\, \mathrm{d}\vec{z} \tag{4.12}$$

across an element with thickness L.

It is common practice to set the displacement field $\vec{D}$ equal to zero inside the piezoelectric material (and not only in the electrodes) of an open circuited PE [13, 5], so that the electric field becomes

$$\vec{E}_{\mathrm{OC}} = -\underline{\varepsilon}^{-1} \underline{d} \vec{\sigma} \tag{4.13}$$

and the voltage becomes

$$V_{\mathrm{PE}}(t) = \int_0^L \underline{\varepsilon}^{-1} \underline{d} \vec{\sigma}\, \mathrm{d}\vec{z} \tag{4.14}$$

Wang et al. [18] write about PZT ceramics and claim (unfortunately without citation or supporting data) that the displacement field is approximately zero under open circuit conditions, which simplifies their PE voltage expression by removing the displacement field term. The common expression

for the voltage generated by a uniaxial stress along the polarisation direction (axis 3) in an open circuited PE is

$$V = g_{33}\sigma_{33}L \tag{4.15}$$

where $g_{33} = d_{33}/\varepsilon_{33}$ is called the piezoelectric voltage constant [5, 7].

If the displacement field is zero ($\vec{D} = 0$) everywhere, both in the electrodes and in the piezoelectric material, Gauss' law eq. (4.5) implies that there is no free charge ($Q_f = 0$) in the PE's electrodes or elsewhere for that matter. In the following calculations of the PE voltage and the free charge present in the PE's electrodes, the displacement field inside the PE will be assumed/approximated to be zero even though it contradicts the presence of free charge.

I suspect that $\vec{D}$ commonly is set to zero in order to reduce the degrees of freedom in the piezoelectric equation eq. (4.2), which makes it possible to analytically calculate a value for the stress based solely on measuring the voltage, and vice versa.

4.3 The capacitance of a stressed, open circuited PE

The amount of free charge at the surface of a dielectric medium is described by its capacity to store free charge at a given voltage across the medium. The capacitance is defined as the ratio of the free charge in the electrodes to the voltage between the electrodes [11]:

$$C \overset{\text{def}}{=} \frac{Q_f}{V} \tag{4.16}$$

For a PE with parallel plate electrodes the capacitance is

$$C = \varepsilon_r\varepsilon_0\frac{A_e}{L} + \frac{A_e\sum_{i=1}^{3} d_{3i}\cdot\sigma_{ii}}{EL} \tag{4.17}$$

This is deduced from Gauss' law eq. (4.5) applied to eq. (4.2), and the voltage eq. (4.12). The first term is constant and can be recognised as the capacitance of parallel plate capacitors without piezoelectric properties.

If the electric field in eq. (4.13) (where $D = 0$ is assumed) is entered into eq. (4.17), the capacitance becomes:

$$C = 2\varepsilon_r\varepsilon_0\frac{A_e}{L} \tag{4.18}$$

Note that this is an unrealistic, self contradicting result, as the capacitance requires that $D \neq 0$. The free charge and the corresponding capacitance is zero when $D = 0$ everywhere.

A different approach to the piezoelectric capacitance is to regard it as a capacitor with varying thickness and electrode area (assuming of course that the PE is not clamped). Ahmad and Allataifeh [6] expressed the capacitance like this:

$$C = \varepsilon_r\varepsilon_0\frac{A_e + \Delta A_e}{L + \Delta L} \tag{4.19}$$

For simplicity, let's assume from here on that the stress term in eq. (4.17) and correspondingly the area and thickness variations in eq. (4.19) are negligible, so that the parallel plate PE's capacitance becomes constant:

$$C = \varepsilon_r\varepsilon_0\frac{A_e}{L} \tag{4.20}$$

The manufacturer of piezoelectric elements, Noliac [1], presents this expression of the PE capacitance, but stresses that it is a crude approximation.

4.4 The electric field in an obliquely stressed, open circuited PE

The electric field in an open circuited PE is

$$\vec{E}_{\mathrm{OC}} = -\underline{\varepsilon}^{-1}\underline{d}\vec{\sigma}$$

when we set the displacement field D to zero in eq. (4.2).

The electric field component of interest is along the polarisation direction (here: the z-axis) between the parallel electrodes:

$$E_z = -\frac{1}{\varepsilon_3}\sum_{i=1}^{3} d_{3i}\cdot\sigma_{ii} \tag{4.21}$$

Note that no shear stress (σ_{ij} where $i \neq j$) is able to produce an electric field along the polarisation axis. For the deduction of the electric field as function of the strain, see appendix B.

Let's assume that a stress pulse traverses the PE at a transmission angle θ_T. Its velocity is

$$\vec{v} = v\cdot\hat{v} = v\cdot(\cos\theta_T\cdot\hat{z} + \sin\theta_T\cdot\hat{y}) \tag{4.22}$$

and correspondingly the longitudinal stress is directed in the same direction as the propagation velocity ($\hat{\sigma} = \hat{v}$).[2] Let's also assume that it is a square pulse with amplitude σ_0. When this stress pulse propagates in the yz-plane, it produces the electric field

$$E_z = -\frac{1}{\varepsilon_3}\sigma_0\cdot(d_{33}\cos\theta_T + d_{32}\sin\theta_T) \tag{4.23}$$

in the PE. θ_T is the angle between the longitudinal stress vector's direction and the PE's polarisation direction. Figure 4.4 plots the relative electric field $E_z(\theta_T)/E_z(0°)$ in a PE made of Noliac NCE56, as function of the transmission angle θ_T.

Equation (4.23) and fig. 4.4 show that there is an angle θ_0 where the PE electric field is zero regardless of the stress amplitude σ_0. Let's call this angle the PE cancellation angle, since the component σ_y cancels out the contribution from σ_z at that angle.

We find the cancellation angle by setting $E_z = 0$ in eq. (4.23):

$$\theta_0 = \arctan\left(-\frac{d_{33}}{d_{32}}\right) \tag{4.24}$$

Note that $d_{32} < 0$ always.

The PE cancellation angle is $\theta_0 = 66.7°$ for Noliac NCE56 [5], where $d_{31} = d_{32} = -250\cdot10^{-12}$ C/N and $d_{33} = 580\cdot10^{-12}$ C/N.

4.5 The voltage across a line-segment of the PE

We will now derive the voltage across a line-segment of a PE before integrating all line-segments in the next section, to get the entire PE's voltage. Let's define a line-segment ξ as a line parallel to the polarisation direction between the two electrodes, at any position y. A line-segment is illustrated in fig. 4.5. The voltage across ξ is

$$V_\xi(y,t) = -\int_0^L \vec{E}(y,z,t)\,\mathrm{d}\vec{z} = -\int_0^L E_z(y,z,t)\,\mathrm{d}z \tag{4.25}$$

[2]The hat marks unity vectors. E.g. $\hat{z}$ is the unity vector in the z-direction.

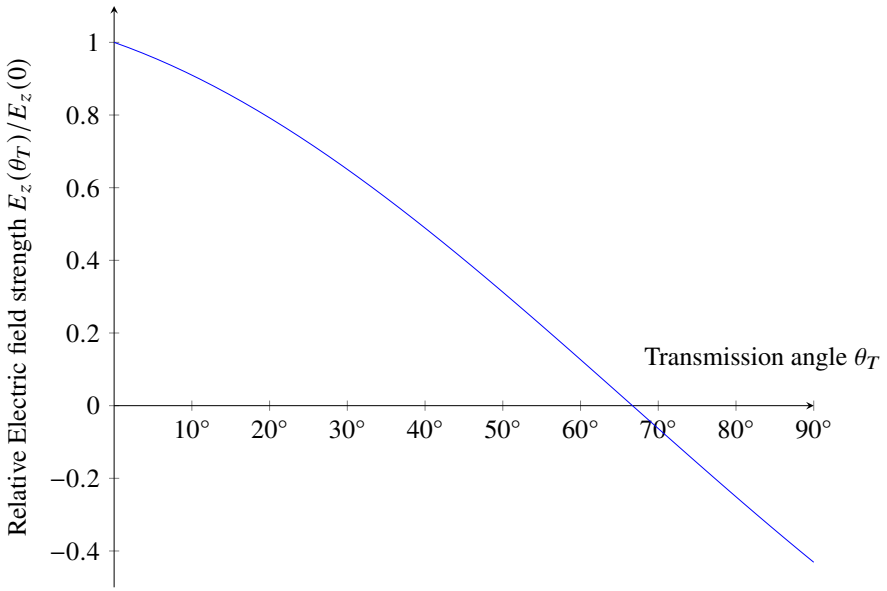

Figure 4.4 *The electric field strength decreases with increasing transmission angle θ_T in a PE. Equation (4.23) is plotted with material constants of Noliac NCE56 [5].*

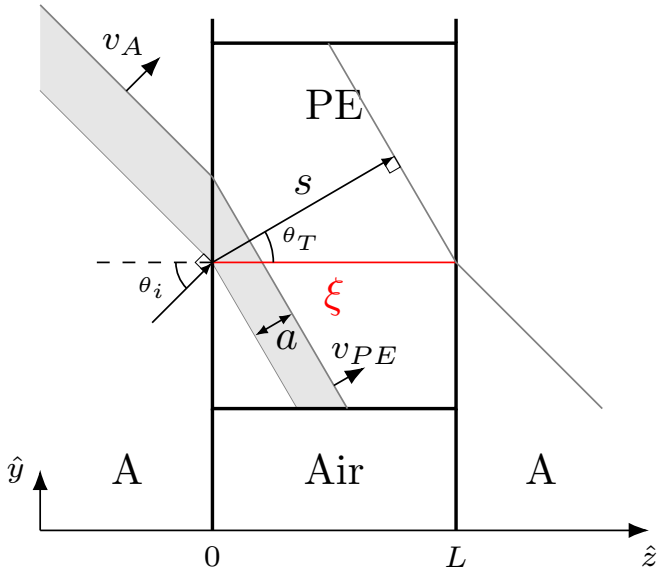

Figure 4.5 *A line-segment ξ (red) is sketched. The PE with thickness L is polarised in the z-direction. The stress pulse (grey region) has pulse length a when it is inside the PE, and propagates at an angle θ_T along the trajectory s. It entered the PE at an incident angle θ_i.*

L is the PE's thickness. When a square stress pulse with amplitude σ_0 traverses the PE at an angle θ_T relative to ξ, the line-integral becomes

$$V_\xi(\theta_T, z(t)) = -\int_0^L E_z \, \mathrm{d}z = -E_z \cdot z(t)$$
$$= \frac{1}{\varepsilon_3}\sigma_0 \cdot z(t) \cdot (d_{33}\cos\theta_T + d_{32}\sin\theta_T) \tag{4.26}$$

where the pulse covers the proportion z/L of the line ξ at time t. This is derived by entering eq. (4.23) into eq. (4.25) and assuming constant stress direction $\hat{\sigma}_0$ and amplitude σ_0 along the entire line ξ (and a correspondingly constant electric field strength E_z). As the stress pulse traverses the line-segment, its maximum voltage during that time is $V_\xi(z = L)$ when the stress pulse length is $a \geq s = L\cos\theta_T$, and $V_\xi(z = a)$ when $a < L\cos\theta_T$.

The maximum voltage of the line-segment ξ as function of transmission angle θ_T relative to when $\theta_T = 0°$, is

$$\frac{V_{\max}(\theta_T)}{V_{\max}(0°)} = (\cos\theta_T + \frac{d_{32}}{d_{33}}\sin\theta_T) \tag{4.27}$$

in the case when $a > L$. When $a < L\cos\theta_T$, less of the line-segment is stressed when $\theta_T = 0°$ than when $\theta_T > 0°$ because we assume an infinitely wide pulse with limited length a. In that case the right side of eq. (4.27) must be multiplied by the fraction $z/a = 1/\cos\theta_T$.

4.6 The voltage across an unevenly stressed PE

Let's now derive the PE's voltage $V(t)$ based on the voltages $V_\xi(y,t)$ across all its line-segments $\xi(y)$. Each line-segment represents an infinitesimally narrow PE (let's call them line-PEs). And these line-PEs are connected in parallel by one common electrode on each side of the PE. When a stress pulse traverses the PE at an angle, some line-segments are stressed before the others. In other words the PE is unevenly stressed across its cross section. Immediately after one line-segment is stressed, a voltage difference occurs between the stressed and the relaxed line-PEs as if they were disconnected. But any voltage difference is quickly evened out because the voltage difference drives a current in the electrode.

Figure 4.6 sketches an equivalent circuit to an unevenly stressed PE. Several line-PEs are initially disconnected to imitate the immediate voltage difference. When the current starts running between parallel connected line-PEs in the PE, it corresponds to closing the switch. The current runs until a voltage equilibrium is established between the line-PEs. In the sketch only one line-PE is initially compressed while the other line-PEs are relaxed. We will now calculate the PE's voltage at equilibrium, using the equivalent circuit in fig. 4.6.

The charge in the circuit is conserved when the switch in fig. 4.6 is opened/closed. For N capacitors

$$Q_i = V_{i,\mathrm{OC}} \cdot C_i \;\; \forall\, i = \{1, 2, ..., N\} \qquad \text{in open circuit (OC)} \tag{4.28}$$

$$Q_{\mathrm{Total}} = V_{\mathrm{CC}} \sum_{i=1}^{N} C_i \qquad \text{in closed circuit (CC) at equilibrium} \tag{4.29}$$

where C_i is the capacitance of each line-PE i. The equilibrium voltage across all capacitors becomes

$$V_{\mathrm{CC}} = \frac{\sum_{i=1}^{N} V_{i,\mathrm{OC}} C_i}{\sum_{i=1}^{N} C_i} \tag{4.30}$$

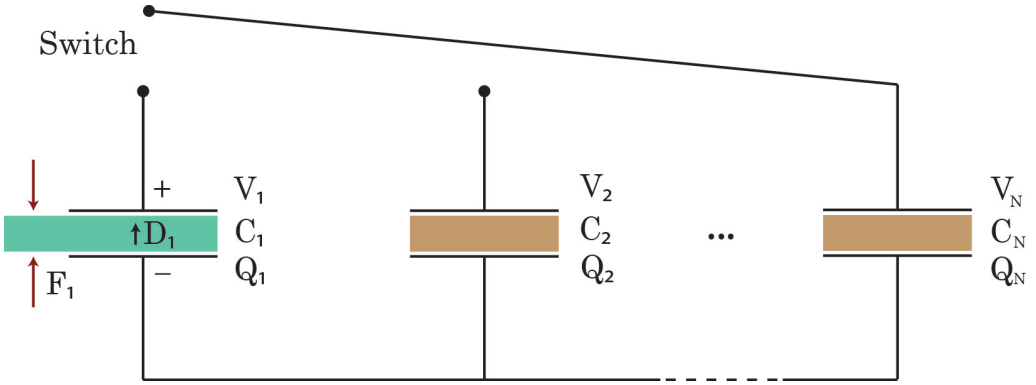

Figure 4.6 This circuit with capacitors is equivalent to a set of line-PEs in open circuit (open switch) and closed circuit (closed switch).

due to charge conservation. This is equivalent to the PE voltage across all parallel connected line-PEs. Notice that this closed circuit voltage is the weighted average of all the open circuit voltages. In the case where all capacitors have equal capacitance $C = C_i \, \forall i$, the closed circuit voltage becomes the average of the open circuit voltages:

$$V_{\mathrm{CC}} = \frac{1}{N} \sum_{i=1}^{N} V_{i,\mathrm{OC}} \tag{4.31}$$

Further, since the line-PEs are infinitesimally narrow (with width $\mathrm{d}y$), the amount of line-PEs N across the entire PE (width B) becomes $N = B/\Delta y \to B/\mathrm{d}y$ and calculus gives that

$$V_{PE}(t) = \lim_{\substack{N\to\infty \\ \Delta y \to \mathrm{d}y}} V_{\mathrm{CC}} = \lim_{\Delta y \to \mathrm{d}y} \frac{1}{B} \sum_{i=1}^{B/\Delta y} V_{i,\mathrm{OC}} \Delta y = \frac{1}{B} \int_0^B V(y,t) \mathrm{d}y \tag{4.32}$$

Equilibrium is reached approximately immediately in a PE, even though the line-PEs are stressed unequally, because there is negligible resistance in the electrode.

The voltage V_{PE} for the entire PE is

$$\begin{aligned}
V_{\mathrm{PE}}(t) &= \frac{1}{B} \int_0^B V(y,t) \, \mathrm{d}y \\
&= -\frac{1}{B} \int_0^B \int_0^L E_z(\vec{r},t) \, \mathrm{d}z \, \mathrm{d}y \\
&= \frac{1}{B\varepsilon_3} \int_0^B \int_0^L \sum_{i=1}^{3} d_{3i} \cdot \sigma_{ii}(\vec{r},t) \, \mathrm{d}z \, \mathrm{d}y \\
&= \frac{1}{B\varepsilon_3} \int_0^B \int_0^L d_{32} \cdot \sigma_{yy}(\vec{r},t) + d_{33} \cdot \sigma_{zz}(\vec{r},t) \, \mathrm{d}z \, \mathrm{d}y \\
&= \frac{L}{\varepsilon_3} (d_{32} \cdot \bar{\sigma}_{yy}(t) + d_{33} \cdot \bar{\sigma}_{zz}(t))
\end{aligned} \tag{4.33}$$

when an arbitrary stress pulse propagates in the yz-plane through an open circuited PE. It is deduced from eq. (4.21) and eq. (4.32). $\bar{\sigma}_{yy}$ and $\bar{\sigma}_{zz}$ are the average stress components, averaged across the entire PE. The PE has thickness L in the polarisation direction along the z-axis, and width B along the y-axis. The PE dimensions L and B are assumed to be constant: any changes to the thickness and width due to the compression or tension, are neglected.

The corresponding free charge that the open circuited PE has capacity to contain, is

$$\begin{aligned} Q_f &= C_{\text{PE}} \cdot V_{\text{PE,OC}} \\ &= \frac{C_{\text{PE}} L}{\varepsilon_3} (d_{32} \cdot \bar{\sigma}_{yy}(t) + d_{33} \cdot \bar{\sigma}_{zz}(t)) \end{aligned} \tag{4.34}$$

This is what the free charge converges towards as $D \to 0$. If the PE has parallel electrodes, the generated PE charge becomes

$$Q_f = A_e \cdot (d_{32} \cdot \bar{\sigma}_{yy}(t) + d_{33} \cdot \bar{\sigma}_{zz}(t)) \tag{4.35}$$

where A_e is the electrode area. The approximate capacitance in eq. (4.20) was entered. Remember that the stress contribution to the PE capacitance in eq. (4.17) has been neglected here.

4.7 The charge generated in open, closed and short circuited PEs

An open and a short circuited PE generate approximately the same amount of free charge if they are equally stressed. The equations eq. (4.10) and eq. (4.35) for short circuited and open circuited PE, respectively, have the same expression for the free charge as function of the stress.

The free charge generated in a stressed PE in a closed circuit with other electrical components (as long as none of them are voltage sources), is equal to the free charge in an open circuited PE if they are equally stressed. The PE is polarised only by stress in this scenario. The circuit in fig. 4.6 sketches capacitors in parallel with a PE. The stressed PE becomes a part of a closed circuit when the switch is closed. The bound charge generated in the PE attracts free charge from elsewhere in the circuit until voltage equilibrium is reached, and the bound charge is generated only by the stress in the PE. Thus the generated free charge is the same for equally stressed PEs regardless of the parallel capacitance that the free charge is distributed to. The extreme cases of short circuited PEs and open circuited PEs correspond to cases where the parallel capacitance goes to infinity and to zero, respectively.

Technically and theoretically speaking, an open circuited PE with electrodes is a PE connected in parallel to a capacitor with a very small capacitance. The outer surfaces of the PE electrodes act as one capacitor.

The general expression for the free charge generated in open, closed and short circuited PEs with parallel electrodes, is

$$Q = Q_f = A_e \sum_{i=1}^{3} d_{3i} \cdot \bar{\sigma}_{ii}(t)) \tag{4.36}$$

when PEs are polarised only by the stress (i.e. a PE in sensor mode). A_e is the electrode area. As mentioned in section 4.2 and section 4.3, this equation is only a crude approximation of the free charge for open circuited PEs.

Note that eq. (4.36) is true only for small stress levels where the linear approximation to the piezoelectric effect holds true; the piezoelectric charge matrix $\underline{d}$ is independent of the stress and the electric field.

For a longitudinal, plane, square stress pulse propagating in the yz-plane ($\sigma_{xx} = 0$) through the PE at an angle θ_T relative to its polarisation direction, the PE generates the free charge

$$Q = \frac{C_{\mathrm{PE}}}{B\varepsilon_3}(d_{33}\cos\theta_T + d_{32}\sin\theta_T)\int_0^B\int_0^L \sigma_0(\vec{r}_{(t)})\,\mathrm{d}z\,\mathrm{d}y \tag{4.37}$$

From here on Q will be called the PE generated (PEG) charge. It is the charge that is generated by the PE and distributed across the electric circuit. It must not to be confused with the PE charge, which is the charge (left) in the PE electrodes.

5 Stressed area coverage

The area that is affected by the stress pulse as it traverses the PE, depends on the pulse's propagation direction. In this chapter we derive the maximum area being stressed by a traversing pulse in the PE as function of the transmission angle θ_T. How the shape of the PEG charge signal's rising edge (as the stress pulse enters the PE) depends on θ_T, will also be studied.

The PEG charge signal is given by the integration of the stress pulse inside the PE at a given time. It is a volume integral, but in case of a plane wave symmetry we can look at the stressed area. Equation (4.37) implies that the charge produced by a square pulse that propagates in the yz-plane, is proportional to the stressed area $A(t)$ at any given time t:

$$Q \propto \int_0^B \int_0^L \sigma_0(\vec{r}_{(t)})\,\mathrm{d}z\,\mathrm{d}y = \sigma_0 \int_0^{y_1(t)} \int_0^{z_1(y,t)} \mathrm{d}z\,\mathrm{d}y = \sigma_0 \cdot A(t) \tag{5.1}$$

5.1 A PE charged by a square pulse via its front entrance

In the case where the PE is not in contact with any ductile material on the side, like in fig. 5.1, the stress pulse enters only at the PE's front.

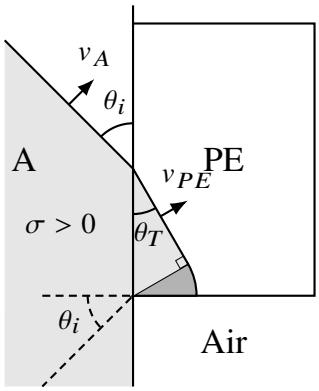

Figure 5.1 Material A and the PE are in contact only at the PE's front. A stress pulse (bright grey area) propagates in material A and is refracted as it's transmitted into the PE due to the difference in mechanical impedance. An area with an expanding stress pulse front (dark grey area) will appear between the refracted plane pulse front's edge and the PE's bottom surface. It spreads out as if from a point source at the corner of the PE, according to Huygens' principle.

The pulse front becomes expansive at the edge because the wave spreads out as if from a point source at the corner of the PE, according to Huygens' principle. This is sketched in fig. 5.1. The stress direction is changed for the expanding pulse front in that region, always pointing in the propagation direction (which is normal to the pulse front). And the energy is conserved in the expansion. The stress amplitude will therefore be smaller there than in the area of the plane wave. At small angles the contribution to the piezoelectric effect from the expanding stress pulse can be neglected. We will neglect this effect even for greater transmission angles, to simplify the calculations. In that case the entire pulse is assumed to propagate in one direction: the refracted

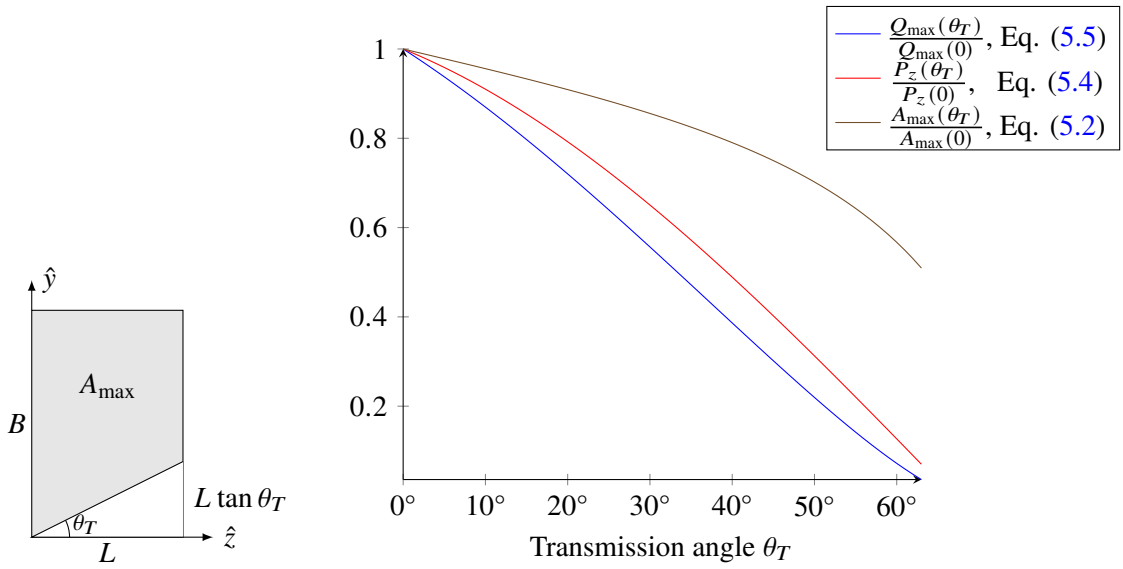

(a) Partially stressed PE

(b) Dimensions of the PE: L=2 mm,B=4 mm. Material data used: Noliac NCE56 [5].

Figure 5.2 The sketched area in (a) is the area traversed by a plane, square stress wave that propagated obliquely from the PE's left side. This area is plotted in (b) as function of the transmission angle θ_T, which is described by eq. (5.2) with $\theta_T < \arctan(B/L) = 63°$. The relative polarisation (see eq. (5.4)) is also plotted. Their product is the curve $\frac{Q_{\max}(\theta_T)}{Q_{\max}(0)}$, according to eq. (5.5).

direction, and leaves an unstressed region (in the shape of a triangle) where the expanding pulse front would have been. Remember that eq. (5.1) assumes unidirectional stress, like in a plane wave.

The maximum area to be covered by an obliquely propagating stress pulse, is sketched in fig. 5.2a. The square pulse is assumed to have an infinite width (or at least wider than the PE), and a finite pulse length $a > Lcos\theta_T$. It propagates at a transmission angle θ_T relative to the z-axis. It covers the area

$$A_{\max}(\theta_T) = \begin{cases} BL - \frac{1}{2}L^2\tan\theta_T, & \text{when } L\tan\theta_T < B \\ \frac{B^2}{2\tan\theta_T}, & \text{when } L\tan\theta_T \geq B \end{cases} \tag{5.2}$$

B is the PE width, and L is its thickness in the z-direction. The maximum stressed area becomes a triangle when the angle θ_T is greater than $\tan^{-1}(B/L)$.

By rewriting the eq. (4.37), the relative maximum PEG charge produced by a longitudinal, plane, square stress pulse becomes

$$\frac{Q_{\max}(\theta_T)}{Q_{\max}(0)} = \frac{A_{\max}(\theta_T)}{A_{\max}(0)} \cdot \frac{P_z(\theta_T)}{P_z(0)} \tag{5.3}$$

where

$$\frac{P_z(\theta_T)}{P_z(0)} = (\cos\theta_T + \frac{d_{32}}{d_{33}}\sin\theta_T) \tag{5.4}$$

Equation (5.3) takes into account two angle dependent factors: the effect of the maximum area stressed in eq. (5.2), and the PE's angle dependent polarisation P. Note that the relative polarisation

is equal to the relative electric field in an open circuited PE, $\frac{P_z(\theta_T)}{P_z(0)} = \frac{E_{z,\mathrm{OC}}(\theta_T)}{E_{z,\mathrm{OC}}(0)}$, which was plotted in fig. 4.4.

When $L\tan\theta_T < B$ the charge becomes

$$\frac{Q_{\max}(\theta_T)}{Q_{\max}(0)} = (1 - \frac{L}{2B}\tan\theta_T)(\cos\theta_T + \frac{d_{32}}{d_{33}}\sin\theta_T) \tag{5.5}$$

as plotted in fig. 5.2b.

The charge signal's shape

The rising edge of the PEG charge signal depends on the increasing PE volume that a stress pulse covers when it enters from one side and traverses the PE. We will continue to assume a plane pulse propagating in the yz-plane. Due to symmetry we only have to consider the area in the yz-plane that the pulse covers. The covered PE area increases in time (the stress pulse enters at $t = 0$):

$$A(t) = \begin{cases} A_1(t), & t \in [0, t_1 = \frac{B\sin\theta_T}{v}] \\ A_1(t_1) + A_2(t - t_1), & t \in [t_1, t_2 = \frac{L}{v\cos\theta_T}] \\ A_1(t_1) + A_2(t_2 - t_1) + A_3(t - t_2), & t \in [t_2, t_2 + \frac{1}{v}(B - L\tan\theta_T)\sin\theta_T] \end{cases} \tag{5.6}$$

where

$$A_1(t) = \frac{(vt)^2}{2\tan\theta_T}$$

$$A_2(t) = \left(B\cos\theta_T - \frac{vt\tan\theta_T}{2}\right)\cdot vt$$

$$A_3(t) = \left(\frac{B - L\tan\theta_T}{\cos\theta_T} - \frac{vt(\tan\theta_T + 1/\tan\theta_T)}{2}\right)\cdot vt$$

Here it is assumed that the stress pulse front reaches the PE's upper left corner (in fig. 5.3a) before it reaches the rear side of the PE. Or put in mathematical terms: $t_1 = \frac{B\sin\theta_T}{v} \leq \frac{L}{v\cos\theta_T} = t_2$ is assumed. This is equivalent to $\sin 2\theta_T \leq \frac{2L}{B}$. The opposite case ($\sin 2\theta_T > \frac{2L}{B}$) causes a slightly different stressed area function. In that case the pulse front reaches the rear side before it reaches the upper left corner $(0, B)$: $A_2'(t) = \frac{L}{\sin\theta_T}\cdot vt$. $A_2'(t)$ is a parallelogram with increasing height vt. The assumption $\tan\theta_T < \frac{B}{L}$ is also made in eq. (5.6). If $L\tan\theta_T > B$, then stage 3 with area $A_3(t)$ disappears.

In this section we have seen how the start of the charge signal is shaped as a stress pulse front traverses the PE at an angle. For comparison, the next section presents the shape of the PEG charge signal due to a stress pulse traversing at zero degree (transmission) angle.

The charge signal of a square stress pulse incident at 0°

The PE charge signal shape is given by the shape, speed and transmission angle θ_T of the traversing stress pulse. For a plane, square pulse traversing the PE at θ_T =0°, the PEG charge signal $Q(z(t))$ becomes a trapezoid, as shown in fig. 5.4. The resulting PEG charge signals of three different pulse lengths a, are presented in the figure: $a > L$, $a = L$ and $a < L$. The stress pulse length and duration t_a are related by the propagation speed v_{PE} in the PE: $a = v_{\mathrm{PE}}\cdot t_a$.

The charge signal's rise time is the stress pulse front's transit time[3] through the PE, when $a > L$. When $a < L$ the rise time is the pulse duration t_a.

[3]Transit time is the time to travel through something.

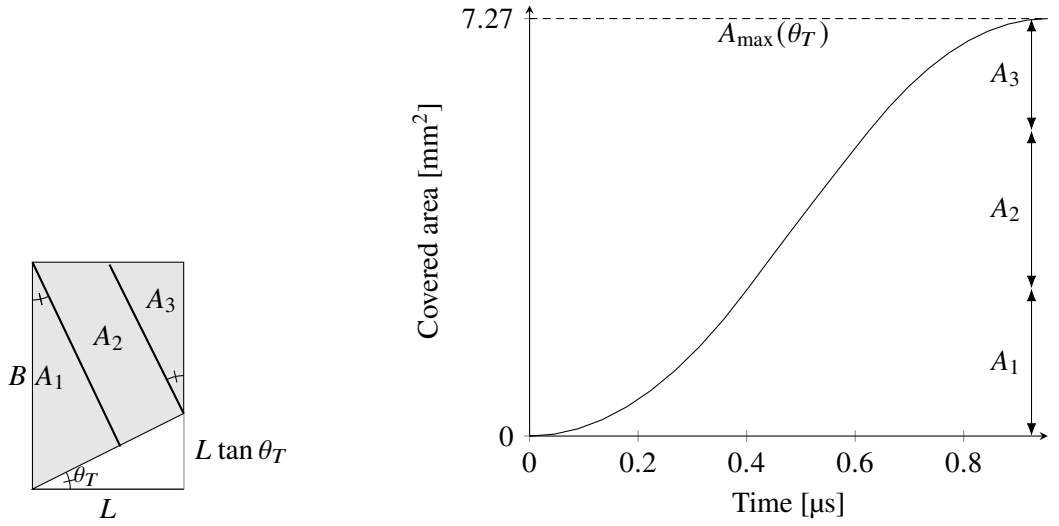

(a) The areas of the three stages in eq. (5.6). (b) Equation (5.6) is plotted for L =2 mm, B =4 mm and θ_T = 20°.

Figure 5.3 The three shaded areas in the PE in (a) are accumulated in the plot in (b) as the stress pulse traverses the PE at an angle θ_T.

The PEG charge for any stress pulse entering at 0° incident angle is

$$Q = C_{\text{PE}} \cdot g_{33} \int_0^L \sigma(z,t)\,\mathrm{d}z \tag{5.7}$$

derived for a uniaxial stress ($\sigma_z \neq 0$, $\sigma_x = \sigma_y = 0$) from eq. (4.37). $g_{33} = \frac{d_{33}}{\varepsilon_3}$ is the piezoelectric voltage constant in the polarisation direction (denoted with index 3). One may notice that eq. (5.7) is equivalent to the cross-correlation between the square pulse and a fixed square function representing the PE with width equal to the PE thickness and with unit amplitude.

5.2 Surface waves contribute to the PE via the free surface

In this study (for simplicity) we neglected the effect of the surface wave that forms on the A-to-air interface when a compressive wave in material A impacts the free surface. This phenomenon is sketched in fig. 5.5. Surface waves in solids are also called Rayleigh waves [16, p. 28]. This surface wave will propagate towards the PE and cause a compressive wave in the PE in addition to the longitudinal wavefront that enters the PE directly. Think of it as a trampoline: Jumping in the centre causes a surface wave to propagate along the sheet out to the sturdy legs at the periphery. The legs are thus pushed down (compressed) by that surface wave. The PE will be compressed by the surface wave just like the legs on a trampoline.

The Rayleigh wave arrives at the PE after the direct longitudinal wave. The Rayleigh wave has to travel farther (i.e. the hypotenuse of a triangle) than the longitudinal wave that created it, and it propagates slower. Rayleigh waves typically propagates slower than shear waves, which are slower than longitudinal waves.[16, p. 40] For example: in steel the Rayleigh wave propagates at 57 % of the longitudinal wave's speed. This is based on the data and equations found in [16, p. 41] and [4].

In addition the creation of the Rayleigh wave as the longitudinal wave hits the free surface, also takes a bit of time.

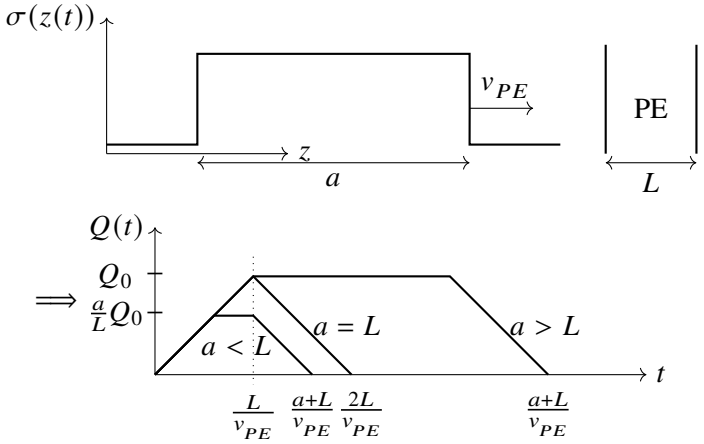

Figure 5.4 The integration of the square stress pulse that propagates through the PE with thickness L, produces one of the charge signals seen below it, depending on the pulse's length a: $a > L$, $a = L$ or $a < L$. The charge signal duration is $\frac{a+L}{v_{PE}}$ for all three cases. The dashed line marks the Gaussian surface S.

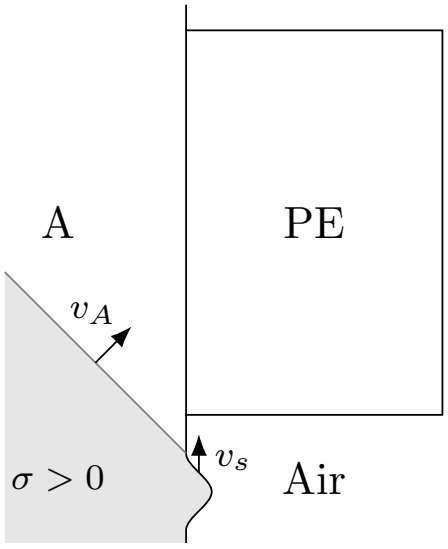

Figure 5.5 A surface wave arises when a longitudinal stress wave in material A impacts the free surface (i.e. the interface to air). The surface wave is going to propagate towards the PE and compress it.

6 The PE generated charge as function of impact angle: A product of the four factors

The previous chapters have presented four angle dependent factors each that affect the charge amplitude of the piezoelectric impact sensor. Now it is time to combine the factors into the product that connects the stress pulse generated at the impact interface, to the PEG charge.

The formula for the relative PEG charge amplitude generated by a longitudinal, plane, square stress pulse, is:

$$\frac{Q_{\max}(\theta_T,\alpha)}{Q_{\max}(0,0)} = I \cdot \frac{T}{T_0} \cdot \frac{A}{A_0} \cdot \frac{P_z}{P_{z,0}} \tag{6.1}$$

$$I = \cos\alpha$$

$$\frac{T}{T_0} = \frac{\frac{Z_A}{Z_{PE}} + 1}{\frac{Z_A}{Z_{PE}}\frac{\cos\theta_T}{\cos\theta_i} + 1}$$

$$\frac{A}{A_0} = 1 - \frac{L}{2B}\tan\theta_T$$

$$\frac{P_z}{P_{z,0}} = \cos\theta_T + \frac{d_{32}}{d_{33}}\sin\theta_T$$

$$\theta_i = \sin^{-1}\left(\frac{v_A}{v_{PE}}\sin\theta_T\right)$$

This is the result of combining the equations for the angle dependent factors: the relative impulse I expressed by eq. (2.3), the isotropic transmission coefficient T expressed by eq. (3.1), the piezoelectric effect that causes polarisation P_z of the PE according to eq. (5.4), and the area A (expressed by eq. (5.2)) that the stress pulse covers as it traverses the PE. The last equation above is Snell's law. Snell's law relates the incident angle θ_i in material A to the transmission angle in the PE. Z_j and v_j are the mechanical impedance and the stress pulse's speed in the indexed material j, respectively. d_{32} and d_{33} are two of the piezoelectric charge constants of the PE. The reference charge $Q_{\max}(0,0)$ is the charge amplitude at 0° impact angle α and 0° transmission angle θ_T.

Equation (6.1) is true for open, closed and short circuited PEs. It describes the relative bound charge generated in the PE, which corresponds to the relative polarisation. When the PE is open circuited, eq. (6.1) is equal to the relative PE voltage amplitude. When the PE is short circuited, eq. (6.1) is equal to the free charge that flows in the current to the PE in order to counter the bound charge and cancel out the electric field that the bound charge causes.

There are several assumptions behind eq. (6.1) that makes it look as simple as it does. The stress pulse being considered is a longitudinal, plane, square shaped pulse with a pulse length and pulse width so great that it can cover the entire PE. A plane wave is an important assumption because it means that the stress is directed in the same direction everywhere in the wave or pulse. And the square shape implies that the same stress amplitude σ_0 is everywhere in the square. In case of non-square pulses the PEG charge amplitude will vary with the portion of the stress pulse that is inside the PE, and is not dividable by a stress amplitude σ_0 and its corresponding reference charge $Q_{\max}(0,0)$. (It may however be approximated as such, specially if the pulse stress gradient is small, i.e. the pulse comprise of long wavelengths.)

Some effects were neglected when deriving eq. (6.1): The expanding part of the wavefront as discussed in section 5.1, and the contribution of the surface wave generated at the free surface next to the PE (see section 5.2).

The maybe most crucial errors in the approximation given by eq. (6.1) are to neglect the effective target thickness in the projectile's direction of flight and the deformation of the impact interface during penetration. As briefly mentioned in chapter 2, these effects are most likely important, but too complex and case dependent to prioritise a quantitative description of it in this analytical, conceptual study. Equation (6.1) is therefore at best valid for the initial pulse before deformation has had time to reshape the projectile and target noticeably. The effective target thickness may be neglected in cases where the target is extremely thick; so thick that the projectile won't perforate it.

Any absorbed energy (due to plastic deformations etc.) in the projectile nose as the pulse traverses it, has not been considered in this study because it is assumed to be an angle independent factor. If the absolute PEG charge amplitude is of interest, the absorbed energy must be taken into account.

Equation (6.1) is also applicable to geometries where the pulse may propagate with incident angle θ_i different from the impact angle α. For projectile nose geometries that generate an expanding longitudinal wave, the equation may approximate the PEG charge amplitude as long as the curvature of the expanding wavefront is small. For instance this is the case for a spherically propagating wave that enters the PE far from its origin. It can be approximated as a plane wave in the PE. The pulse may still have to be square shaped or at least a pulse with minor variations in stress amplitude (like a sound wave with long wavelength), if the eq. (6.1) is expected to make a good approximation of the PEG charge amplitude.

More complex projectile geometries cause more complex waves where the longitudinal stress may point in all directions and vary significantly in amplitude. These situations will most likely have a more complicated relative PEG charge than eq. (6.1). Simulation tools are recommended for those cases, where eq. (4.33) can be applied to the average stress of the simulated PE. Remember to adjust the PE's elasticity according to the electric circuit it is thought to be connected to.

6.1 Applying the analytic solution to a real-world example

We will now take a look at a simple scenario designed to fulfil all the assumptions of the derived PEG charge in eq. (6.1). The projectile and target are designed to ensure that the stress pulse stays plane and square throughout the entire journey from the impact interface to and through the PE.

This scenario mainly demonstrates the derived PEG charge expression to gain understanding of how impact sensors work. However, it also resembles the specific, real impact case where the straight side of a conically shaped projectile nose tangents a flat surface (like the top of a tank) and generates a shock wave given that the impact is hard enough.

Shock waves only appear at stress levels above the material's elastic limit (also known as yield strength in metals) [9]. As presented in chapter 2, the stress is proportional to the impulse and the area of impact. For a given target and projectile, the projectile is shocked above a certain impact velocity.

A shock wave can be approximated as a square stress pulse, as argued in more detail in appendix C. A shock wave is defined by the steepness of its wavefront. Its front is almost vertical (strain rate $\gtrapprox 10^7$ s^{-1} [16, p. 325]), thus shocking the material. (When shocked, the material's state jumps to a higher energy state without following the curve of its equilibrium states [9].)

In fig. 6.1 a longitudinal, plane, square stress pulse is produced at the flat impact interface and propagates towards the PE, where it generates a charge with the relative amplitude as presented in fig. 6.2. The projectile's "tilted square" shape ensures that the stress pulse is unchanged as it

propagates from the impact interface to the PE.[4] Hence it enters the PE in a longitudinal, plane and square shape. The wavefront enters the PE at the same angle as the impact angle: $\alpha = \theta_i$. The PE is polarised in the z-direction.

The mechanical constants used in this scenario for material A (steel) and the PE (Noliac NCE56), are found in table 3.1. The piezoelectric constants of Noliac NCE56 are found in [3].

The curves in fig. 6.2 present the relative PE charge amplitude for (a) an open and (b) a short circuited PE made of Noliac's NCE56 material. The relative charge for a closed circuited PE will lie somewhere between those curves, depending on the electric impedance of the closed circuit.

The difference between the curves (a) and (b) is caused by the relative transmission coefficient $\frac{T}{T_0}$ and most of all the refraction $\frac{\sin\theta_i}{\sin\theta_T}$, as they depend on the PE's elasticity. A short circuited PE is softer than an open circuited PE, due to different electric fields. This is deduced in appendix A. Hence an open and a closed circuited PE are stressed differently and therefore generate different amounts of charge.

Piezoelectric elements are anisotropic (typically orthotropic). The isotropic transmission coefficient used in eq. (6.1) therefore introduces an error. However, when the Young's modulus in all directions are approximately equal ($Y_1 = Y_2 \approx Y_3$), the error can be neglected. In this example Noliac NCE56 is applied as PE material. Its Young's moduli are related as $Y_3/Y_1 = 0.9$ [3].

[4] Cerv et al. [8] calculated the elastic waves in two, colliding infinite rods with cylinder symmetry. According to their calculations the wavefront is plane in those rods, but there are trailing waves that initially are spherical. Far into the (thin) rods these trailing waves will converge into a plane wavefront.

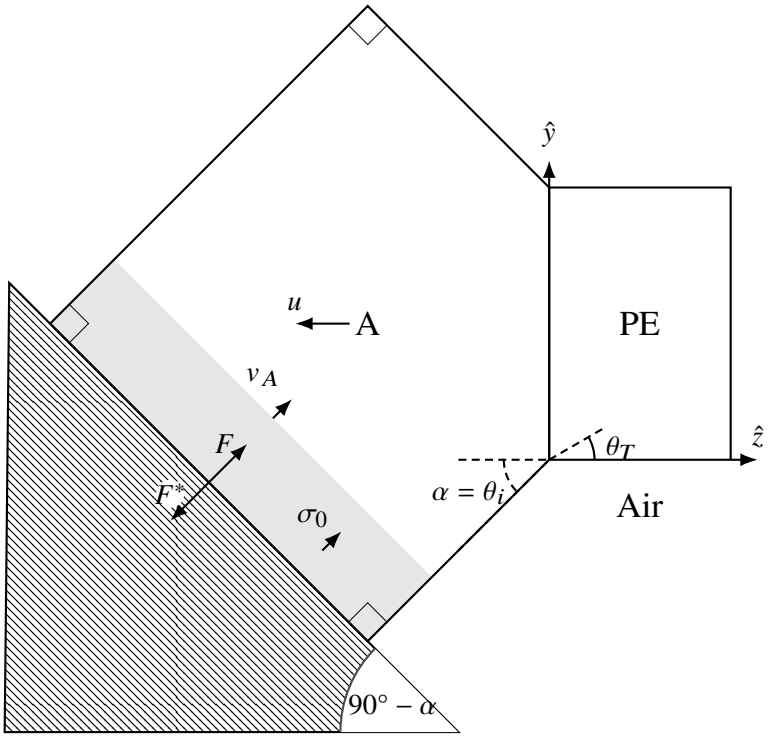

Figure 6.1 *An oblique impact situation generating a longitudinal, plane stress pulse: The tilted square shaped projectile nose impacts a target plate at an angle α. $\vec{u}$ is the projectile velocity prior to impact. The projectile nose A is a square rotated at an angle $\theta_i = \alpha$ in order to generate a plane wave at the plane impact interface, and to have orthogonal walls that lead the pulse unchanged to the PE.*

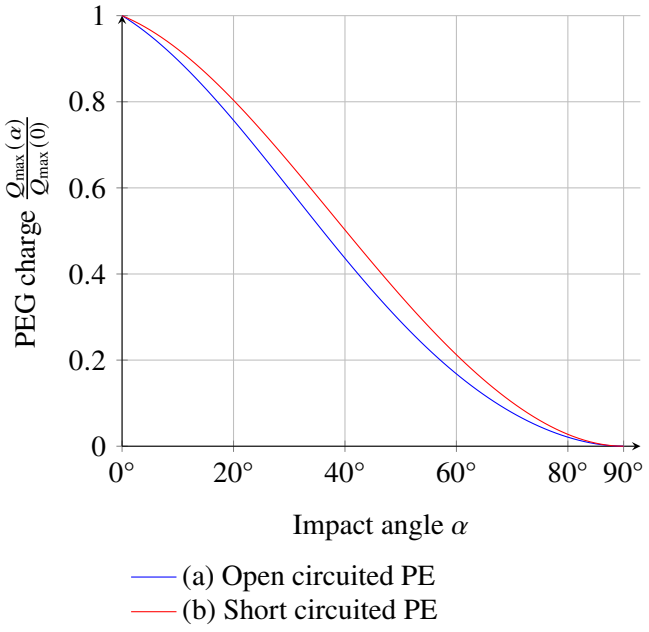

Figure 6.2 *The relative PE generated charge amplitude of the scenario sketched in fig. 6.1 is plotted, which is described by eq. (6.1) with $\alpha = \theta_i$. Material A is steel and the PE is NCE56. See table 3.1 for mechanical constants. The PE's dimensions: L=2 mm, B=4 mm. The piezoelectric charge constants used, are $d_{33} = 580 \cdot 10^{-12}$ m/V and $d_{31} = -250 \cdot 10^{-12}$ m/V [3].*

7 Conclusion

The PE generated charge depends on both the stress amplitude and propagation direction through it. A general expression has been derived for the free charge generated by an incoming stress pulse in a PE with parallel plate electrodes: eq. (4.36). It makes no assumption about the characteristics of the stress pulse that enters the PE. The equation (4.36) applies to unevenly stressed PEs in an open, closed or short circuit. However, it is a crude approximation for open circuited PEs because the displacement field is assumed to be negligible when calculating the voltage, and the stress contribution to the PE capacitance is neglected. These assumptions are discussed in section 4.2 and section 4.3. The voltage across an unevenly stressed, open circuited PE was also deduced (see eq. (4.33)) based on that same displacement field assumption.

The impact angle dependency of the PE generated charge amplitude has been derived (see eq. (6.1)), where the PE was traversed by a longitudinal, plane, square stress pulse. The equation was applied to a conceptual impact scenario that was designed so that the assumptions of the derived equation were (approximately) true. The resulting relative PE charge amplitude as function of the impact angle, was presented in fig. 6.2. It decreases with increasing impact angle. The relative PE charge amplitude for an open and a closed circuited PE, are quite similar. At 60° impact angle the PE charge amplitude is $Q_{\max}(60°) \approx 0.2 \cdot Q_{\max}(0°)$. At 90° it is zero.

Four factors were taken into consideration when deriving the relative PE charge and voltage amplitude as function of impact angle, each presented in their own chapter. These factors are: the impact impulse, the transmission coefficient, the proportion of the PE volume that effectively is stressed by the pulse, and the piezoelectric effect which depends on the pulse's amplitude and propagation direction through the PE.

Some effects were disregarded when deriving the relative PE charge amplitude. It should be noted that two of them were not considered negligible to the impact angle dependency of the PE charge amplitude, only too complex and too case specific to be quantified in this analytical, conceptual study. These two effects were the effective target thickness and the size of the impact interface area as function of impact angle. The stress' effect on the capacitance of piezoelectric elements was also neglected, but should be considered in future work when calculating the free charge generated by open and closed circuited PEs.

References

[1] Dictionary. Technical report, Noliac.

[2] Piezo basics - tutorial. Technical report, Noliac. Version 1604.

[3] PZT Materials complete properties. Technical report, CTS, August 2018.

[4] Material data sheet steel grade -34crnimo6. Technical report, Ovako, info@ovako.com, 2019. (https://steelnavigator.ovako.com/steel-grades/34crnimo6/ Accessed on 30.10.2019).

[5] Noliac Ceramics NCE datasheet. http://www.mmech.com/images/stories/Technologies/Piezo%20Ceramics/Noliac_CEramics_NCE_datasheet_1404.pdf, 2019.

[6] Mahmoud Al Ahmad and Areen Allataifeh. Electrical extraction of piezoelectric constants. 4(11):e00910, nov 2018.

[7] Rodney D Caudle and George B Clark. Experiments on the measurement of the response of rock to dynamic loads. Technical report, MISSOURI UNIV-ROLLA SCHOOL OF MINES AND METALLURGY, 1963.

[8] J. Cerv, V. Adamek, F. Vales, D. Gabriel, and J. Plesek. Wave motion in a thick cylindrical rod undergoing longitudinal impact. *Wave Motion*, 66:88 – 105, 2016.

[9] Paul Cooper. *Explosives Engineering*. Wiley-Blackwell, 1996.

[10] Ravinder S Dahiya and Maurizio Valle. *Robotic tactile sensing: technologies and system*. Springer, 2013.

[11] Richard Feynman, Robert Leighton, and Matthew Sands. *The Feynman Lectures on Physics, Volume II*. Basic Books, Hachette Book Group, 1290 Avenue of the Americas, New York, NY 10104, 2011. accessed on https://www.feynmanlectures.caltech.edu/II_10.html on 25.11.2021.

[12] J. F. Haskins and J. S. Hickman. A derivation and tabulation of the piezoelectric equations of state. 22(5):584–588, sep 1950.

[13] Hyeoung Woo Kim, Shashank Priya, Kenji Uchino, and Robert E Newnham. Piezoelectric energy harvesting under high pre-stressed cyclic vibrations. *Journal of Electroceramics*, 15(1):27–34, March 2005.

[14] W. P. Mason. First and second order equations for piezoelectric crystals expressed in tensor form. *The Bell System Technical Journal*, 26(1):80–138, 1947.

[15] C. C. Mei. Chapter three: Two dimensional waves. https://web.mit.edu/1.138j/www/material/chap-3.pdf, 2004. The MIT course "Wave Propagation".

[16] Marc A Meyers. *Dynamic behavior of materials*. John Wiley & sons, 1994.

[17] Jayant Sirohi and Inderjit Chopra. Fundamental understanding of piezoelectric strain sensors. *Journal of Intelligent Material Systems and Structures*, 11, April 2000.

[18] Ruizhi Wang, Enling Tang, and Guolai Yang. Dynamic piezoelectric properties of PZT-5h under shock compression. *physica status solidi (a)*, 216(6):1800859, feb 2019.

[19] Marek-Adam Weber, Marc Kamlah, and Dietrich Munz. *Experimente zum Zeitverhalten von Piezokeramiken*. Number 6465. FZKA, 2000.

[20] Dayu Zhou. *Experimental investigation of non-linear constitutive behavior of PZT piezoceramics*. Number 6869. FZKA Bunia, 2003.

A The relation between an open and a short circuited PE's stiffness matrix

In PE datasheets two types of elastic compliance coefficients are usually presented: Open (s_D) and short (s_E) circuit. The annotations mean: Displacement field $\vec{D} = 0$ in open circuit PEs, while the electric field $\vec{E} = 0$ in short circuited PEs.

When the displacement field D is zero, eq. (4.2) can be rewritten as

$$\vec{E} = -\underline{\varepsilon}^{-1}\underline{d}\vec{\sigma} \tag{A.1}$$

We get the constitutive relation between stress and strain in an open circuit case by replacing the electric field E in eq. (4.1) with eq. (A.1):

$$\begin{aligned}\vec{S} &= \underline{s}\vec{\sigma} + \underline{d}^T\vec{E} \\ &= (\underline{s} - \underline{d}^T\underline{\varepsilon}^{-1}\underline{d})\vec{\sigma} \\ &= \underline{s}_D\vec{\sigma}\end{aligned}$$

The relation between the elastic compliance matrix of an open and a short circuited PE, is

$$s_D = \underline{s}_E - \underline{d}^T\underline{\varepsilon}^{-1}\underline{d}. \tag{A.2}$$

It is defined according to [2], which allegedly follows the European standard EN-50324-2. For the three first diagonal elements in the matrix ($s_{ii}\,\forall\, i = \{1, 2, 3\}$) the electromechanical coupling factor k can be used to relate the open and closed circuit: $s_{D,ii}/s_{E,ii} = (1 - k_{ii}^2)$.

Note that the elastic compliance s_D relates strain to stress in open circuited PEs. $\underline{s}_D$ is not the $\underline{s}$ in eq. (4.1) with annotation added.While $s = s_E$ in eq. (4.1) because the index E means that $\vec{E} = 0$.

For closed circuits with some resistance (not short circuit), the PE's elasticity will lie somewhere between s_E and s_D.

Equation (A.2) shows that an open circuited PE is stiffer than in a short circuited PE: $Y_{D,i} = 1/s_{D,ii} > Y_{E,i} = 1/s_{E,ii} \forall\, i = \{1, 2, 3\}$. Young's moduli Y_i are the three first diagonal elements of an inversed elastic compliance matrix (s^{-1}). The permittivity ε is positive, and so are the diagonal elements of the elastic compliance matrices s_E and s_D.

B PE voltage as function of strain

An alternative to calculating the piezoelectric field from stress (see eq. (4.33)), is to calculate it from strain.

The strain is related directly to electric field in the piezo as

$$E_3 \left(\sum_{k=1}^{3} \sum_{i=1}^{3} d_{3i} \cdot (s^{-1})_{ik} \cdot d_{3k} - \varepsilon_{33} \right) = \sum_{j=1}^{3} \sum_{i=1}^{3} d_{3i} \cdot (s^{-1})_{ij} \cdot S_j \tag{B.1}$$

This is deduced from the piezoelectric equations and assuming that displacement field $\vec{D} = 0$ (open circuit):

$$\begin{aligned} \vec{S} &= \underline{s}\vec{\sigma} + \underline{d}^T \vec{E} \\ -\underline{\varepsilon}\vec{E} &= \underline{d}\vec{\sigma} \end{aligned}$$

By rewriting these equations and solving for strain and electric field, the result becomes

$$\underline{ds}^{-1}\vec{S} = \underline{d}\vec{\sigma} + \underline{ds}^{-1}\underline{d}^T\vec{E} = -\underline{\varepsilon}\vec{E} + \underline{ds}^{-1}\underline{d}^T\vec{E} = (-\underline{\varepsilon} + \underline{ds}^{-1}\underline{d}^T)\vec{E} \tag{B.2}$$

Strain $\vec{S}$ and stress $\vec{\sigma}$ are both 6×1 vectors according to the Voigt notation: $\vec{\sigma} = [\sigma_1, \sigma_2, \sigma_3, \sigma_4, \sigma_5, \sigma_6]^T = [\sigma_x, \sigma_y, \sigma_z, \sigma_{yz}, \sigma_{zx}, \sigma_{xy}]^T$ and likewise for strain. The last three elements are shear elements. The electric field $\vec{E} = [E_1, E_2, E_3]^T = [E_x, E_y, E_z]^T$, where E_3 is oriented along the PE's polarisation.

Sirohi and Chopra [17] presents typical matrices for piezoelectric elements (IEEE Standard, 1987). The permittivity matrix $\underline{\varepsilon}$ is a diagonal matrix with $\varepsilon_1, \varepsilon_2$ and ε_3 as entries. For piezoelectric elements like PZT, the piezoelectric charge constant matrix $\underline{d}$ is

$$\underline{d} = \begin{bmatrix} 0 & 0 & 0 & 0 & d_{15} & 0 \\ 0 & 0 & 0 & d_{24} & 0 & 0 \\ d_{31} & d_{32} & d_{33} & 0 & 0 & 0 \end{bmatrix} \tag{B.3}$$

Elastic compliance matrix[5]

$$\underline{s} = \begin{bmatrix} s_{11} & s_{12} & s_{13} & 0 & 0 & 0 \\ s_{21} & s_{22} & s_{23} & 0 & 0 & 0 \\ s_{31} & s_{32} & s_{33} & 0 & 0 & 0 \\ 0 & 0 & 0 & s_{44} & 0 & 0 \\ 0 & 0 & 0 & 0 & s_{55} & 0 \\ 0 & 0 & 0 & 0 & 0 & s_{66} \end{bmatrix} \tag{B.4}$$

First we derive the right-hand side of eq. (B.1). When multiplying eq. (B.3) by the inverse of $\underline{s}$ in eq. (B.4), we get

$$\underline{d}\,\underline{s}^{-1} = \begin{bmatrix} 0 & 0 & 0 & 0 & d_{15} \cdot s_{55}^{-1} & 0 \\ 0 & 0 & 0 & d_{24} \cdot s_{44}^{-1} & 0 & 0 \\ \sum_{i=1}^{3} d_{3i} \cdot (s^{-1})_{i1} & \sum_{i=1}^{3} d_{3i} \cdot (s^{-1})_{i2} & \sum_{i=1}^{3} d_{3i} \cdot (s^{-1})_{i3} & 0 & 0 & 0 \end{bmatrix} \tag{B.5}$$

[5]Elastic compliance matrix is the inverse stiffness matrix, so linear elasticity is assumed. The diagonal elements s_{11}, s_{22} and s_{33} are the inverse Young's moduli in three directions.

We further multiply it by the strain vector $\vec{S}$ and the third element of the vector is the right-hand side of eq. (B.1):

$$\underline{d}\,\underline{s}^{-1}\,\vec{S} = [d_{15}\cdot(s^{-1})_{55}\cdot S_5, d_{24}\cdot(s^{-1})_{44}\cdot S_4, \sum_{j=1}^{3}\sum_{i=1}^{3} d_{3i}\cdot(s^{-1})_{ij}S_j]^T \tag{B.6}$$

$$= \begin{bmatrix} d_{15}\cdot s_{55}^{-1}\cdot S_5 \\ d_{24}\cdot s_{44}^{-1}\cdot S_4 \\ \sum_{j=1}^{3}\sum_{i=1}^{3} d_{3i}\cdot(s^{-1})_{ij}\cdot S_j \end{bmatrix} \tag{B.7}$$

Now, let's derive the left-hand side of eq. (B.1). We first multiply eq. (B.5) by the transposed $\underline{d}$ in eq. (B.3):

$$\underline{d}\,\underline{s}^{-1}\,\underline{d}^T = \begin{bmatrix} d_{15}^2(s^{-1})_{55} & 0 & 0 \\ 0 & d_{24}^2(s^{-1})_{44} & 0 \\ 0 & 0 & \sum_{k=1}^{3}\sum_{i=1}^{3} d_{3i}\cdot(s^{-1})_{ik}\cdot d_{3k} \end{bmatrix} \tag{B.8}$$

When further multiply it by the electric field, we get the left-hand side of eq. (B.1):

$$\underline{d}\,\underline{s}^{-1}\,\underline{d}^T\cdot\vec{E} = \tag{B.9}$$

$$\begin{bmatrix} d_{15}^2 s_{55}^{-1}\cdot E_1 \\ d_{24}^2 s_{44}^{-1}\cdot E_2 \\ \sum_{k=1}^{3}\sum_{i=1}^{3} d_{3i}\cdot(s^{-1})_{ik}\cdot d_{3k}\cdot E_3 \end{bmatrix} \tag{B.10}$$

If we enter eq. (B.9) and eq. (B.6) into eq. (B.2), the third element on both sides of the equation is eq. (B.1). $\mathbb{Q}.\mathbb{E}.\mathbb{D}$.

Uniaxial, elastic stress

In case of a uniaxial, elastic stress, the PE voltage as function of the axial strain S becomes

$$V = E_{33}L = \frac{\sum_{j=1}^{3}\sum_{i=1}^{3} d_{3i}\cdot(s^{-1})_{ij}\cdot(-r)^{1-\delta_{3j}}}{(\sum_{k=1}^{3}\sum_{i=1}^{3} d_{3i}\cdot(s^{-1})_{ik}\cdot d_{3k}) - \varepsilon_{33}}\cdot S_3\cdot L \tag{B.11}$$

$r = -S_1/S_3$ is the Poisson ratio, and the elasticity is assumed to be orthotropic ($s_{31} = s_{32} \neq s_{33}$). s_{ij}^{-1} is the ij-th element in the inverse elastic compliance matrix $\underline{s}^{-1}$. δ_{kj} is the Kronecker delta. Note that E_3 is the electric field in the polarisation direction. Stiffness matrix is the inverse elastic compliance matrix. Young's modulus $Y = s_{ii}^{-1}$ for $i = \{1, 2, 3\}$.

C Shock waves are approximately square pulses

The shock wave can be approximated as a square pulse as long as it is close to the free surface where the pulse's rear edge originated. The shock wavefront is always regarded as vertical as a square pulse front, while the rear edge's slope declines as the shock wave propagates.

A shock wavefront is by definition approximately vertical. Estimated strain rates for shock fronts (in solids) are in the order of $[10^7, 10^9]$ s^{-1} [16, p. 325]. Shock waves in solids appear above the material's elastic limit (also known as yield strength in metals). The upper limit of the expected rise time for a passing shock wavefront can be calculated based on the strain at the elastic limit. For example: the strain at the yield strength of steel SS2541 is $\varepsilon_{\text{yield}} = \sigma_{\text{yield}}/Y = 4.3\,\text{mm/m}$ [4]. As a result the rise time of a shock wavefront is shorter than $\varepsilon/\dot{\varepsilon} = \frac{4.3\,\text{mm/m}}{10^7\ \text{s}^{-1}} = 0.43\,\text{ns}$ and the corresponding "rise length" at the order of 1 µm.[6]

The rear edge of a shock pulse is called the relief wave [9]. The material is relieved from compressed (or stretched) state in that relief wave. The relief process from a shocked state follows the Hugoniot-Rankine equation of (equilibrium) states (EOS), while the shocking process is a jump between two states in this EOS. The different locations or phases in the relief wave have different wave velocities because they are in different states. Therefore the relief wave will become wider in time. Over time the slope becomes gentler. Close to the origin of the relief wave (typically free surfaces where stress can be relieved), the slope is still steep, and the rear edge can be approximated as vertical.

The relief wave will catch up with the shock wavefront after some time [9]. It propagates slightly faster than the shock wave. In this report the PE voltage amplitude due to a square stress pulse, is investigated. The PE must be located close enough to the impact interface (or more precisely: close to the target's free surface) in order to approximate a shock wave as a square pulse. However, when deriving the PE voltage amplitude as function of impact angle, the pulse is only required to cover the PE with the proportion of the pulse that has constant amplitude. The derived PE voltage amplitude in present report may therefore apply to a shock wave as long as the shock wavefront leaves the PE before the relief wave enters it.

[6] The length of a shock wavefront in steel SS2541 is shorter than $5.2\,\text{km/s} \cdot 0.43\,\text{ns} = 2.2\,\mu\text{m}$.

About FFI

The Norwegian Defence Research Establishment (FFI) was founded 11th of April 1946. It is organised as an administrative agency subordinate to the Ministry of Defence.

FFI's mission

FFI is the prime institution responsible for defence related research in Norway. Its principal mission is to carry out research and development to meet the requirements of the Armed Forces. FFI has the role of chief adviser to the political and military leadership. In particular, the institute shall focus on aspects of the development in science and technology that can influence our security policy or defence planning.

FFI's vision

FFI turns knowledge and ideas into an efficient defence.

FFI's characteristics

Creative, daring, broad-minded and responsible.

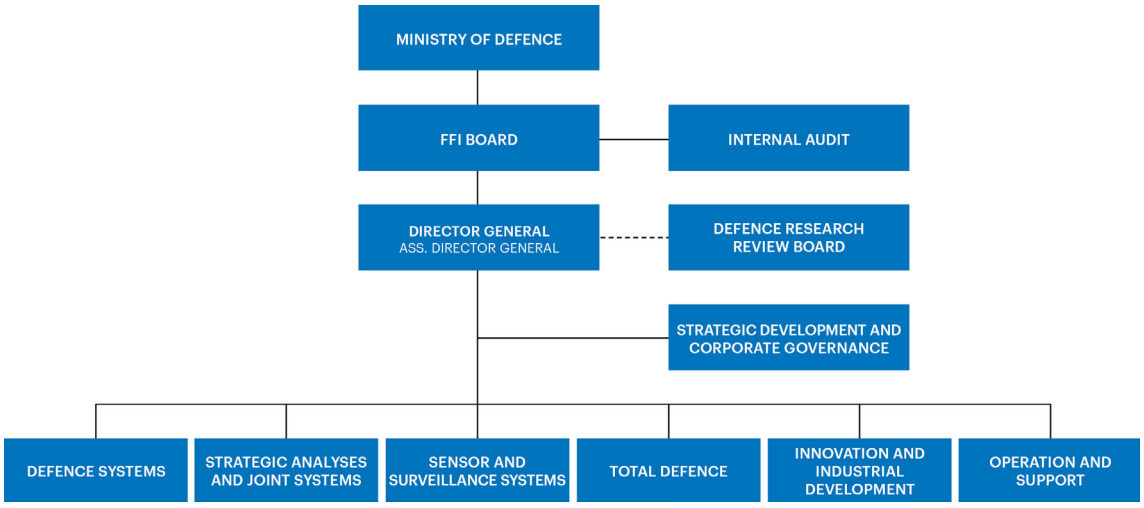

Forsvarets forskningsinstitutt
Postboks 25
2027 Kjeller

Besøksadresse:
Instituttveien 20
2007 Kjeller

Telefon: 63 80 70 00
Telefaks: 63 80 71 15
Epost: post@ffi.no

Norwegian Defence Research Establishment (FFI)
P.O. Box 25
NO-2027 Kjeller

Office address:
Instituttveien 20
N-2007 Kjeller

Telephone: +47 63 80 70 00
Telefax: +47 63 80 71 15
Email: post@ffi.no